Berk, M., Špačková, O., & Straub, D. (2017). Probabilistic Design Storm method for improved flood estimation in ungauged catchments. Water Resources Research, 53. DOI: 10.1002/2017WR020947

To view the published open abstract, go to https://doi.org/10.1002/2017WR020947.

Probabilistic Design Storm Method for Improved Flood Estimation in Ungauged Catchments

Mario Berk[1], Olga Špačková[1], Daniel Straub[1]

[1]Engineering Risk Analysis Group, Technische Universität München, Germany

mario.berk@tum.de, olga.spackova@tum.de, straub@tum.de

Key Points:

- A novel Probabilistic Design Storm method for flood estimation in ungauged basins is proposed based on structural reliability methods.
- Proposed methodology overcomes the average recurrence interval neutrality assumption of the standard design storm approach.
- The effect of multiple correlated rainfall durations on flood frequencies can be accounted for with the Probabilistic Design Storm method.

Abstract

The design storm approach with event-based rainfall-runoff models is a standard method for design flood estimation in ungauged catchments. The approach is conceptually simple and computationally inexpensive, but the underlying assumptions can lead to flawed design flood estimations. In particular, the implied average recurrence interval (ARI) neutrality between rainfall and runoff neglects uncertainty in other important parameters, leading to an underestimation of design floods. The selection of a single representative critical rainfall duration in the analysis leads to an additional underestimation of design floods. One way to overcome these non-conservative approximations is the use of a continuous rainfall-runoff model, which is associated with significant computational cost and requires rainfall input data that are often not readily available. As an alternative, we propose a novel Probabilistic Design Storm method that combines event-based flood modelling with basic probabilistic models and concepts from reliability analysis, in particular the First-Order Reliability Method (FORM). The proposed methodology overcomes the limitations of the standard design storm approach, while utilizing the same input information and models without excessive computational effort. Additionally, the Probabilistic Design Storm method allows deriving so called Design Charts, which summarize representative design storm events (combinations of rainfall intensity and other relevant parameters) for floods with different return periods. These can be used to study the relationship between rainfall and runoff return periods. We demonstrate, investigate and validate the method by means of an example catchment located in the Bavarian Pre-Alps, in combination with a simple hydrological model commonly used in practice.

Keywords: Design storm approach; First Order Reliability Method; Flood Frequency; Flood exceedance probability; Design flood; Probabilistic Design Storm method

1 Introduction

The estimation of a design flood, represented by an annual maximum peak discharge with a fixed return period (often the 100-year event), is an important task in engineering hydrology. Design flood estimates are used for flood risk management and for the design of structures such as dams, bridges, culverts or dykes. In many catchments, discharge measurements are not available as a basis for a statistical estimation of design floods. One class of methods to estimate design floods in these ungauged catchments utilizes regionalization of flood frequencies from gauged basins [*Shaw et al.*, 2011]. More frequently, in ungauged basins, rainfall-runoff models are utilized to derive design floods from rainfall statistics. Among these, the design storm approach is the most commonly used method in ungauged basins for determining design floods in engineering practice [*Pathiraja et al.*, 2012].

The broad use of the design storm approach is due to its simplicity and low computational cost, as well as the availability of input rainfall data in form of Intensity Duration Frequency (IDF) or Depth Duration Frequency (DDF) curves, which are provided by meteorological services in most countries. With this approach, a rainfall input of a specific return period is transformed to a peak discharge using event-based rainfall-runoff models [*Viglione et al.*, 2009]. The two major assumptions underlying the classical design storm approach are [*Rahman et al.*, 2002]: 1) the corresponding rainfall-runoff events fulfill average-recurrence-interval (ARI) neutrality, which signifies that the return periods of concurrent rainfall and peak discharge are assumed to be the same, and 2) the design flood of a given return period can be estimated based on a single critical rainfall duration, i.e. the rainfall duration that generates the highest peak discharge. The first assumption is only a rough approximation because a rainfall event with a given return period leads to different peak discharges in function of other random parameters, such as the temporal rainfall pattern, antecedent wetness or spatial rainfall variability [*Shaw et al.*, 2011; *Verhoest et al.*, 2010]. The second assumption neglects the possible contribution of rainfall events of different durations on flood exceedance probabilities. As a results of these approximations, the design storm approach tends to underestimate flood probabilities [*Viglione et al.*, 2009; *Grimaldi et al.*, 2012b; *Li et al.*, 2014; *Awadallah et al.*, 2015].

The use of continuous rainfall-runoff models allows avoiding both assumptions underlying the design-storm concept [*Camici et al.*, 2011]. A continuous time series of rainfall data is used as the model input, and the resulting discharge time series is statistically analyzed to determine the design flood with the target return period. This approach has been widely used in the scientific literature [*Calver and Lamb*, 1995; *Cameron et al.*, 1999; *Cameron et al.*, 2000; *Lamb and Kay*, 2004; *Haberlandt et al.*, 2008; *Blazkova and Beven*, 2009; *Grimaldi et al.*, 2012a; *Pathiraja et al.*, 2012; *Rogger et al.*, 2012]. Its major drawbacks are the high computational costs to simulate long time series of discharges in high temporal resolution and the need for sophisticated stochastic rainfall models to generate the rainfall time series as model input. Approaches to reduce computational cost have been proposed [*Paquet et al.*, 2013; *Lawrence et al.*, 2014; *Li et al.*, 2014]. Nevertheless, in data scarce regions, the discharge data required to calibrate some of the rainfall-runoff models as well as the rainfall data to calibrate and the know-how to implement stochastic rainfall generators are not readily available. The approach is thus rarely used in practice.

Probabilistic extensions of the design storm approach have been proposed in the literature that allow overcoming the assumption of ARI neutrality. They mostly use Monte Carlo Simulation (MCS) to model the uncertainty in the event-based rainfall-runoff model parameters. [*Loukas et al.*, 1996] and [*Loukas*, 2002] consider the uncertainty in the temporal rainfall distribution and the infiltration abstraction parameter; [*Aronica and Candela*, 2007] combine a random rainfall depth of the critical rainfall duration with uncertainty in antecedent moisture conditions and a semi-distributed SCS-CN approach; [*Rahman et al.*, 2002] use probabilistic rainfall duration, rainfall intensity, rainfall pattern and initial loss; [*Svensson et al.*, 2013] include the uncertainty in the rainfall duration, intensity, temporal pattern, inter-event arrival time, the initial flow and soil moisture. The SHYREG method [*Arnaud et al.*, 2015] models the uncertainty in the number of relevant rainfall events per year and generates these with a stochastic hourly rainfall generator. Like the continuous models, these approaches therefore require either a joint probabilistic model of rainfall duration and intensity or the utilization of rainfall generators for obtaining the rainfall inputs. Additionally, MCS is inefficient for modeling of events with high return period, which might lead to prohibitively large computational costs if an advanced rainfall-runoff model is used.

In this paper, we propose an alternative methodology, termed Probabilistic Design Storm method, which corresponds to a probabilistic extension of the design flood estimation with an event-based rainfall-runoff model. It uses as inputs the readily available IDF/DDF curves for describing extreme rainfall events, which should make it easily applicable in engineering practice. The methodology is based on formulating the design flood estimation problem within a reliability analysis framework. In particular, it uses FORM (First-Order Reliability Method) [*Rackwitz*, 2001; *Der Kiureghian*, 2005] for evaluating the design flood, which is computationally efficient and provides useful insights into the importance of the input uncertainties.

Reliability analysis aims at estimating the probability of rare events, which classically correspond to failures of a structure or a system [*Melchers*, 1999; *Straub*, 2014]. In the context of the design flood estimation, the rare event is the exceedance of a design flood. The corresponding annual exceedance probability is fixed (e.g. at 10^{-2} for the 100-year event), and the corresponding rare event (i.e. the design flood) is sought. This corresponds to an inverse reliability problem [*Winterstein et al.*, 1993]. A reliability-based formulation of the peak discharge estimation has been introduced by [*Melching*, 1992], who uses FORM for computations. The analysis was made for a given rainfall event; the rainfall magnitude was therefore not considered as uncertain. FORM was furthermore applied by [*Awadallah et al.*, 2015] in combination with the SCS-CN hydrological model to account for the uncertain rainfall-runoff model parameters and evaluate their effect on flood exceedance probabilities; however, only a single rainfall duration was considered.

A major issue in probabilistic extensions of the design storm approach, which has not been dealt with previously, is that rainfalls of different durations can lead to the same design flood. In the standard deterministic design storm approach, this is not an issue; it is sufficient to select the most critical rainfall duration. In a probabilistic context, this approach leads to an underestimation of the probability of exceeding a discharge level Q. Every rainfall duration can lead to Q, albeit with smaller probability than the critical one. Neglecting this possibility leads to an underestimation of the exceedance probability associated with Q, and hence to an underestimation of the design flood. As we demonstrate in this paper, system reliability analysis provides a straightforward answer to this challenge. By conceptually considering different rainfall durations as different mechanisms that can lead to the same rare event (the exceedance of the discharge level Q), the problem is equivalent to the reliability analysis of a series system, for which standard solutions are available [*Der Kiureghian*, 2005].

In contrast to continuous simulations, the proposed method is computationally sufficiently efficient to be used in standard engineering applications. However, it is conceptually more demanding than the classical design storm approach; direct practical implementation would thus be fostered by implementation in a software package. Alternatively, the proposed approach can be used for calibrating the parameters of the classical design storm approach, similarly to [*Camici et al.*, 2011], who used a continuous model for this purpose. To facilitate such a calibration and easy implementation in practice, we propose the use of *design charts* for recommending the optimal combination of input parameters to the deterministic design storm approach. The design charts display the most likely input parameter combinations to produce a discharge of a given return period. They can thus be interpreted as representative design scenarios for the design storm method.

To perform numerical investigations, we implement the proposed methodology to a case study at the Trauchgauer Ach in Bavaria, Germany. We evaluate the modeling choices and compare the obtained results to the classical design storm approach and a flood frequency analysis of measured stream flow data, which illustrates the effects of the ARI neutrality assumption and the use of a critical rainfall duration.

2 Methodology

We introduce a Probabilistic Design Storm (PDS) approach for design flood estimation using event-based rainfall runoff models. First, a reliability-based formulation of the design flood problem is presented in Section 2.1. This formulation allows to account for multiple uncertainties in input parameters in the rainfall-runoff model, additionally to the random rainfall intensity. The choice of uncertain input parameters depends on the applied rainfall-runoff model; examples are soil moisture, temporal rainfall pattern, time of concentration, infiltration, interception and catchment vegetation. In Section 2.2, the principles of deriving IDF and DDF curves are described, which are important for understanding the relevance of multiple rainfall durations in the analysis. In Section 2.3, we propose a framework for including multiple rainfall durations in the probabilistic model. Computational methods to analyze the model are outlined in Section 2.4, particularly FORM. Section 2.5 introduces design charts as a tool to make use of the results of the Probabilistic Design Storm method in the standard design storm approach. In Section 2.6 the hydrological model implemented in the case study is summarized.

2.1 Interpreting the design flood in the context of reliability analysis

The design flood problem consists of defining the discharge that corresponds to a given return period. The 100-year event q_{100} corresponds to the annual maximum discharge Q with exceedance probability 1/100, i.e. $\Pr(Q > q_{100}) = 10^{-2}$ in any year. In ungauged basins, Q is estimated in function of (random) input parameters $\mathbf{X}$ using a hydrological model.

The design flood problem is formulated within the reliability analysis framework, which aims at estimating probabilities of rare events. Here, the extreme event is $\{Q(\mathbf{X}) > q\}$, exceedance of a discharge q. For fixed model input parameters $\mathbf{X} = \mathbf{x}$, Q is evaluated with the hydrological model and the event either occurs or does not. Therefore, $\{Q(\mathbf{X}) > q\}$ corresponds to a domain in the outcome space of the input random variables, as illustrated in Figure 1. Exemplarily, the shaded area is the domain of $\{Q(\mathbf{X}) > 30 \text{ m}^3/\text{s}\}$. In reliability analysis, this is known as the failure domain. The probability of the rare event is

$$\Pr(Q(\mathbf{X}) > q) = \int_{q-Q(\mathbf{X})\leq 0} f_{\mathbf{X}}(\mathbf{x})\, \mathrm{d}\mathbf{x} \tag{1}$$

where $f_{\mathbf{X}}(\mathbf{x})$ is the joint Probability Density Function (PDF) of the input random variables $\mathbf{X}$. The integral computes the probability of being in the failure domain (the shaded domain of Figure 1).

The boundary between the failure domain and the remaining outcome space is termed the limit state surface (LSS). It is mathematically defined by

$$q - Q(\mathbf{X}) = 0 \tag{2}$$

In Figure 1, multiple limit state surfaces corresponding to different q's are shown.

A variety of methods have been developed in the structural reliability community to efficiently solve integrals of the form given in Eq. (1). These include FORM, tailored importance sampling schemes, subset simulation and other sequential Monte Carlo methods [*Melchers*, 1999; *Straub*, 2014].

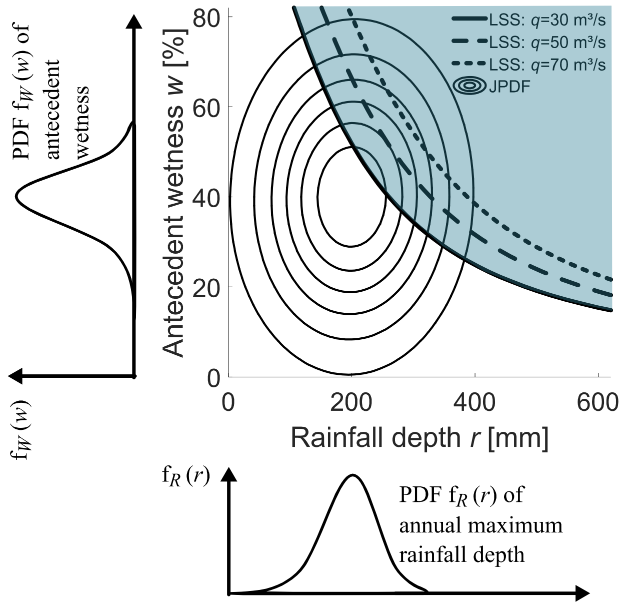

Figure 1. Illustration of the reliability formulation of the design flood estimation for two uncertain input variables $\mathbf{X} = [R; W]$: Rainfall depth R and antecedent wetness W. The shaded area corresponds to the event of the annual maximum discharge exceeding $q = 30\ \mathrm{m}^3/s$. Additional limit state surfaces corresponding to different extreme discharges are also shown. As an example, a rainfall of 400 mm with an antecedent wetness of 50% will lead to a discharge in excess of $70\ \mathrm{m}^3/\mathrm{s}$. The same rainfall with an antecedent wetness of 30% will lead to a discharge in excess of $30\ \mathrm{m}^3/s$ but below $50\ \mathrm{m}^3/s$.

To find a design flood q_T with return period T, an inverse problem must be solved, in which the probability is fixed at $1/T$ and the threshold q_T is found by the equality:

$$\Pr(Q(\boldsymbol{X}) > q_T) = 1/T \tag{3}$$

To avoid repeatedly solving the integral of Eq. (1), inverse FORM can be employed to determine q_T. Details are provided in Section 2.4.4.

2.2 Analysis of rainfall data (IDF/DDF analysis)

Statistical analysis of rainfall data is performed for fixed rainfall durations by means of a moving window approach, which allows to derive IDF/DDF curves [*Mays*, 2005; *Malitz*, 2005; *Viglione et al.*, 2009]. The analysis is briefly reviewed in the following because it is crucial for understanding the treatment of different rainfall durations in the probabilistic model introduced in Section 2.3. We focus here on DDF, but the analysis is analogous for IDF.

The moving window approach proceeds as follows: from the rainfall data (typically available in hourly resolution), time series of d-hourly rainfall sums are extracted. This gives at each time the total rainfall depth in the following d-hour interval. Then, in an Extreme Value (EV) analysis, the annual maximum rainfall depths associated with different durations are extracted from each time series. A probabilistic model is fitted to these extracted annual maxima. Rainfall depths associated with specific return periods in function of rainfall duration are determined from these curves by interpolation; these are displayed in the form of DDF curves.

When analyzing rainfall data with the moving window approach, annual maximum rainfall depths associated with different durations can arise from the same storm event, i.e. the corresponding moving windows can overlap. As a consequence, it is to be expected that the annual maxima for different rainfall durations are correlated, in particular for similar durations. This correlation can be found empirically, as exemplarily illustrated in Figure 2. Annual maxima associated with a 1-hour and a 3-hour duration are highly correlated, whereas those associated with a 1-hour and a 12-hour duration exhibit only a mild correlation.

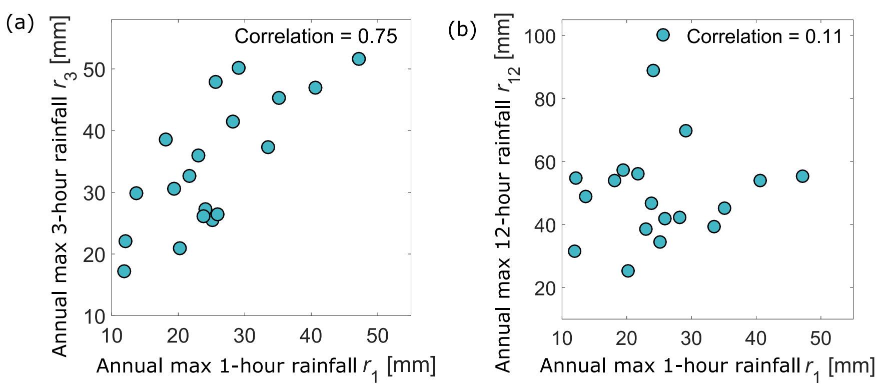

Figure 2. Scatter plot of annual maxima for rainfall depths of durations: (a) 1-hour and 3-hour; (b) 1-hour and 12-hour. (a) shows strong correlation, whereas (b) is only weakly correlated. The data has been recorded at rain gauge Hohenpeißenberg [*DWD*, 2015], see also Section 3.2.5.

Because the moving window approach is central to the widely utilized rainfall statistics in form of IDF/DDF, all input parameters to an event-based hydrological model must be interpreted with the same underlying definition of the rainfall durations. For example, it has to be distinguished between a soil moisture parameter associated with a 1-hour duration and one associated with a 12-hour duration of the rainfall event.

In the next section, we describe how the correlation in the different durations and input parameters can be accounted for in a Probabilistic Design Storm (PDS) approach.

2.3 Modeling multiple rainfall durations

An annual maximum discharge of value q can be caused by rainfalls of different durations. Hence, also the discharges are associated with different moving time windows. In a probabilistic setting – unlike in the standard deterministic design storm approach – it is not possible to identify a single critical rainfall duration. Instead, it is necessary to jointly consider multiple rainfall durations and the associated discharges.

To formalize, let $Q_d(\mathbf{X}_{\boldsymbol{d}})$ denote the annual maximum discharge associated with duration d, computed with an event-based hydrological model with model input $\mathbf{X}_{\boldsymbol{d}} = [X_{d,1}, \dots, X_{d,j}, \dots, X_{d,m}]$, with m being the number of model parameters for a single duration. These parameters consist of the annual maximum rainfall depth or intensity of duration d and the additional inputs to the hydrological model, which are associated with the same moving window duration. Common values for d are 1 h, 3 h, 6 h, …, 72 h, but the choice may depend on catchment size and characteristics. The annual maximum discharge is

$$Q(\mathbf{X}) = \max_{d} Q_d\,(\mathbf{X}_{\boldsymbol{d}}) \tag{4}$$

with $\mathbf{X} = [\mathbf{X}_{d_1}, \dots, \mathbf{X}_{d_n}]$. n is the number of durations considered. The corresponding probability of the annual maximum discharge exceeding a value q is

$$\Pr(Q(\mathbf{X}) > q) = \Pr\left[\left(Q_{d_1}\left(\mathbf{X}_{\boldsymbol{d_1}}\right) > q\right) \cup \left(Q_{d_2}\left(\mathbf{X}_{\boldsymbol{d_2}}\right) > q\right) \cup \dots \cup \left(Q_{d_n}\left(\mathbf{X}_{\boldsymbol{d_n}}\right) > q\right)\right] \tag{5}$$

In system reliability, this corresponds to a series system of n components, whose failure events are $\left\{Q_{d_i}\left(\mathbf{X}_{\boldsymbol{d_i}}\right) > q\right\}$. One can therefore make use of the available methods and results for such systems.

As discussed in Section 2.2, the annual maximum rainfalls and additional input parameters associated with the different moving window durations are correlated. This correlation among the input parameters $\mathbf{X} = [\mathbf{X}_{d_1}, \dots, \mathbf{X}_{d_n}]$ is described with the correlation matrix $\mathbf{R}_{\mathbf{X}}$ whose size is $(n \times m) \times (n \times m)$. Due to $\mathbf{R}_{\mathbf{X}}$, also the failure events $\left\{Q_{d_i}\left(\mathbf{X}_{\boldsymbol{d_i}}\right) > q\right\}$ and $\left\{Q_{d_k}\left(\mathbf{X}_{\boldsymbol{d_k}}\right) > q\right\}$ are correlated with an $n \times n$ correlation matrix $\boldsymbol{\rho}$. The computation of Eq. (5) is described in Section 2.4.

Without any knowledge about the correlation $\boldsymbol{\rho}$ of the different exceedance events $\left\{Q_{d_i}\left(\mathbf{X}_{\boldsymbol{d_i}}\right) > q\right\}$, bounds on the probability $\Pr(Q(\mathbf{X}) > q)$ can be found as follows [*Ditlevsen*, 1979]:

$$\max_{i}\left[\Pr\left(Q_{d_i}\left(\mathbf{X}_{\boldsymbol{d_i}}\right) > q\right)\right] \le \Pr(Q(\mathbf{X}) > q) \le \sum_{i=1}^{n} \Pr\left(Q_{d_i}\left(\mathbf{X}_{\boldsymbol{d_i}}\right) > q\right) \tag{6}$$

The lower bound is in analogy to the deterministic design storm approach: The probability is taken as the one associated with the moving window rainfall duration leading to the highest exceedance probability. This result would be exact if all exceedance events $\left\{Q_{d_i}\left(\mathbf{X}_{\boldsymbol{d_i}}\right) > q\right\}$ were fully dependent, i.e. if they were all associated with the same storm event. The upper bound occurs if the exceedances $Q_{d_i}\left(\mathbf{X}_{\boldsymbol{d_i}}\right) > q$ were mutually exclusive, i.e. if they would all occur in different years. This is clearly unrealistic. For practical purposes, an alternative upper bound could be used, based on the (generally conservative) assumption of statistical independence among different exceedance events:

$$\Pr(Q(\mathbf{X}) > q) \leq 1 - \prod_{i=1}^{n}\left[1 - \Pr\left(Q_{d_i}\left(\mathbf{X}_{\boldsymbol{d_i}}\right) > q\right)\right] \tag{7}$$

To keep the methodology as general as possible, we consider the wider bound of Eq. (6) in the following, but note that the narrower upper bound of Eq. (7) should be applicable in practice. In addition, in Section 2.4.3 we outline a method for (approximately) computing the probability according to Eq. (5) if the correlation $\mathbf{R_X}$ among the input random variables $\mathbf{X} = [\mathbf{X}_{d_1}, \dots, \mathbf{X}_{d_n}]$ is known.

2.4 Computing exceedance probabilities

We first present an efficient solution for computing the exceedance probability for a single rainfall duration d, $\Pr(Q_d(\mathbf{X}_{\boldsymbol{d}}) > q)$, according to Eq. (1). By computing $\Pr\left(Q_{d_i}\left(\mathbf{X}_{\boldsymbol{d_i}}\right) > q\right)$ for all relevant durations d_i, the overall exceedance probability can be estimated based on the bounds provided in the previous section. In Section 2.4.3, the solution for a single rainfall duration is extended to computing the $\Pr(Q(\mathbf{X}) > q)$ directly according to Eq. (5).

2.4.1 First-order reliability method (FORM)

FORM is applied for computing $\Pr(Q_d(\mathbf{X}_{\boldsymbol{d}}) > q)$ according to Eq. (1). As its name implies, FORM is based on a first-order Taylor expansion of the model output [*Rackwitz and Fiessler*, 1978]. To achieve a good approximation, the first-order approximation is performed in a transformed space of independent standard normal random variables $\mathbf{U}_{\boldsymbol{d}}$. To this end, it is convenient to express the event of interest $\{Q_d(\mathbf{X}_{\boldsymbol{d}}) > q\}$ by means of a so-called limit state function:

$$g_d(\mathbf{X}_{\boldsymbol{d}}) = q - Q_d(\mathbf{X}_{\boldsymbol{d}}) \tag{8}$$

The limit state function $g_d(\mathbf{X}_{\boldsymbol{d}})$ is defined such that occurrence of the event corresponds to $g_d(\mathbf{X}_{\boldsymbol{d}})$ taking a negative value. It is $\{g_d(\mathbf{X}_{\boldsymbol{d}}) < 0\} = \{q - Q_d(\mathbf{X}_{\boldsymbol{d}}) < 0\} = \{Q_d(\mathbf{X}_{\boldsymbol{d}}) > q\}$.

An equivalent limit state function G_d in standard normal space is obtained by a probability-conserving transformation $\mathbf{U}_{\boldsymbol{d}} = T_U(\mathbf{X}_{\boldsymbol{d}})$. With T_U^{-1} denoting the inverse transform, G_d is obtained as:

$$G_d(\mathbf{U}_{\boldsymbol{d}}) = g_d[T_U^{-1}(\mathbf{U}_{\boldsymbol{d}})] = q - Q_d[T_U^{-1}(\mathbf{U}_{\boldsymbol{d}})] \tag{9}$$

Any joint distribution of $\mathbf{X}_d$ can be transformed to independent standard normal $\mathbf{U}_d$. In the simplest case, when all $\mathbf{X}_d$ are independent, the random variables can be transformed individually by

$$T_U: U_{d,j} = \Phi^{-1}\left[F_{X_{d,j}}\left(X_{d,j}\right)\right], \qquad j = 1, \dots, m. \tag{10}$$

$F_{X_{d,j}}$ is the cumulative distribution function (CDF) of $X_{d,j}$; Φ is the standard normal CDF and Φ^{-1} its inverse. The corresponding inverse transformation is

$$T_U^{-1}: X_{d,j} = {F_{X_{d,j}}}^{-1}\left[\Phi\left(U_{d,j}\right)\right], \qquad j = 1, \dots, m. \tag{11}$$

If the $\mathbf{X}_d$ are dependent and belong to the Gaussian copula class, the Nataf transformation is applicable, which is summarized in the appendix [*Der Kiureghian and Liu*, 1986]. For general dependence models, the Rosenblatt transformation can be applied, which transforms the random variables sequentially by utilizing the conditional distributions [*Hohenbichler and Rackwitz*, 1981].

While these transformations are essential to FORM, they are also beneficial for a multitude of other structural reliability methods [*Rackwitz*, 2001; *Papaioannou et al.*, 2015]. Details on these transformations can be found in textbooks [*Ditlevsen and Madsen*, 1996; *Melchers*, 1999]. A Matlab routine for this transformation (ERADist) is available from www.era.bgu.tum.de/software.

Because the transformation to U-space is probability conserving, the probability of the rare event can be computed by integrating over the corresponding failure domain in U-space, $G(\mathbf{U}_d) \leq 0$. Eq. (1) is therefore rewritten to

$$\Pr(Q_d(\mathbf{X}_d) > q) = \int_{g_d(\mathbf{X}_d)\leq 0} f_{\mathbf{X}_d}(\mathbf{x}_d)\,\mathrm{d}\mathbf{x}_d = \int_{G_d(\mathbf{U}_d)\leq 0} \varphi_m(\mathbf{u}_d)\,\mathrm{d}\mathbf{u}_d, \tag{12}$$

wherein φ_m is the m-dimensional independent standard normal PDF.

The limit state function $G_d(\mathbf{U}_d)$ is approximated by a first-order Taylor expansion around the so-called design point $\mathbf{u}_d^*$. This is the value of $\mathbf{u}_d$ in the failure domain (i.e. complying with $G_d(\mathbf{u}_d) \leq 0$) with the largest probability density, i.e. the mode of $\varphi_m(\mathbf{u}_d)$ conditional on $G_d(\mathbf{u}_d) \leq 0$. Because φ_m is rotation-symmetric around the origin, $\mathbf{u}_d^*$ can be found by a geometric optimization problem:

$$\mathbf{u}_d^* = \arg\min\|\mathbf{u}_d\| \quad \text{subject to} \quad G_d(\mathbf{u}_d) \leq 0 \tag{13}$$

$\|\mathbf{u}_d\| = \sqrt{{\mathbf{u}_d}^T\mathbf{u}_d}$ is the Euclidean norm of $\mathbf{u}_d$.

The design point $\mathbf{u}_d^*$ has size m. The linear approximation of the limit state function around $\mathbf{u}_d^*$ is termed G_d' and illustrated in Figure 3. β_d' denotes the Euclidian distance from the origin to the design point:

$$\beta_d' = \|\mathbf{u}_d^*\| \tag{14}$$

The marginal distribution of $\mathbf{U}_d$ in the direction from the origin to the design point is the standard normal distribution. Therefore, the probability of $G_d'(\mathbf{U}_d) \leq 0$ is equal to the probability of a standard normal random variable taking a value less than $-\beta_d'$, as illustrated in Figure 3.

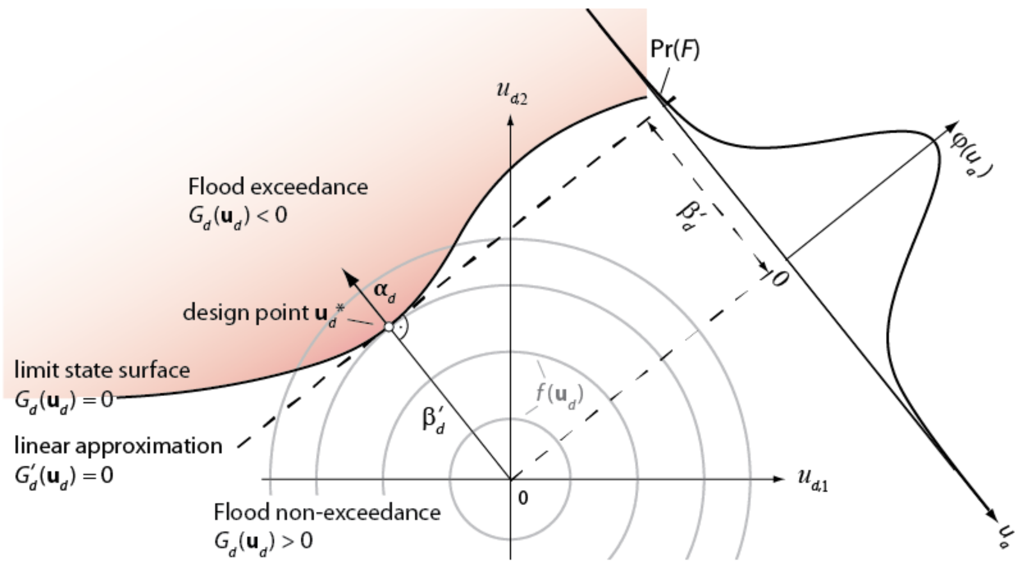

Figure 3. Illustration of the FORM approximation in standard normal space with two random variables $U_{d,1}$ and $U_{d,2}$. The linear approximation is performed at the design point $\mathbf{u}_d^*$ at a distance β_d' from the origin. U_a is the direction perpendicular to the linearized limit state surface $G_d'(\mathbf{U}_d) = 0$. The probability of $G_d'(\mathbf{U}_d) \leq 0$ is equal to the probability of $U_a \leq -\beta_d'$. Since U_a, has the standard normal distribution, $\Pr(G_d'(\mathbf{U}_d) \leq 0)$ is given by Eq. (15).

The FORM approximation of the probability $\Pr(Q_d(\mathbf{X}_d) > q) = \Pr(G_d(\mathbf{U}_d) \leq 0)$ is thus

$$\begin{aligned} \Pr(Q_d(\mathbf{X}_d) > q) &= \Pr(G_d(\mathbf{U}_d) \leq 0) \\ &\approx \Pr(G_d'(\mathbf{U}_d) \leq 0) \\ &= \Phi(-\beta_d'). \end{aligned} \tag{15}$$

In this relation lies the strength of FORM: Once the design point is identified, the FORM estimate of $\Pr(Q_d(\mathbf{X}_d) > q)$ is readily obtained. For this reason, β_d' is known as the FORM reliability index.

In most applications, the limit state function around the design point $\mathbf{u}_d^*$ is only mildly non-linear in standard normal space. Further away from the design point, the approximation may be poor, but as long as the number of relevant random variables in $\mathbf{X}_d$ is not too large, the probability mass is concentrated near $\mathbf{u}_d^*$; the poor quality of the approximation away from $\mathbf{u}_d^*$ is thus not relevant. For this reason, the FORM approximation is surprisingly accurate for a wide range of problems [*Rackwitz*, 2001].

2.4.2 Sensitivity measures

A major advantage of FORM is that it directly provides information about the sensitivity of the probability of flood exceedance to the input random variables. This information is contained in the normalized negative gradient row vector $\boldsymbol{\alpha}_d$ of the design point $\mathbf{u}_d^*$ [*Der Kiureghian*, 2005]:

$$\boldsymbol{\alpha}_d = -\frac{\nabla G_d(\mathbf{u}_d^*)}{\|\nabla G(\mathbf{u}_d^*)\|} \tag{16}$$

$\nabla G_d(\mathbf{u}_d^*)$ is the gradient of G_d at the design point. $\boldsymbol{\alpha}_d$ is a unit vector of dimension m, pointing from the origin to the design point (see Figure 3). Its components $\alpha_{d,j}$ can be computed directly from the components $u_{d,j}^*$ of the design point vector $\mathbf{u}_d^*$:

$$\alpha_{d,j} = \frac{u_{d,j}^*}{\beta_d'} \tag{17}$$

$\alpha_{d,j}$ is an indicator for the influence of the random variable $X_{d,j}$ on the probability of flood exceedance associated with duration d. The larger its absolute value $|\alpha_{d,j}|$, the larger its influence on $\Pr(Q_d(\mathbf{X}_d) > q)$. It is $\sum_j \alpha_{d,j}^2 = 1$, so that the sensitivity is often expressed by $\alpha_{d,j}^2$. Input random variables with small $|\alpha_{d,j}|$ can be replaced by a deterministic value with little loss of accuracy, e.g. the uncertainty of a random variable $X_{d,j}$ with $\alpha_{d,j} = 0.1$ contributes only $\alpha_{d,j}^2 = 1\%$ to the probability of failure.

2.4.3 Combining multiple rainfall durations for computing flood exceedance probabilities

For each considered rainfall duration $d = d_i$, the corresponding FORM analysis is performed to compute $\Pr(Q_{d_i}(\mathbf{X}_{d_i}) > q)$ and the associated sensitivities $\alpha_{d_i,j}$. On this basis, bounds on the flood exceedance probability $\Pr(Q(\mathbf{X}) > q)$, which take all n durations into account, can be evaluated following Eq. (6) or (7).

As an alternative, system reliability analysis with FORM also enables the direct computation of $\Pr(Q(\mathbf{X}) > q)$ according to Eq. (5). Noting that the formulation in Eq. (5) corresponds to the reliability analysis of a series system, the FORM approximation of $\Pr(Q(\mathbf{X}) > q)$ is, in analogy to [*Hohenbichler and Rackwitz*, 1982; *Der Kiureghian*, 2005], found as

$$\Pr(Q(\mathbf{X}) > q) \approx 1 - \Phi_n(\mathbf{b}; \boldsymbol{\rho}). \tag{18}$$

Φ_n is the multivariate standard normal CDF with correlation coefficient matrix $\boldsymbol{\rho}$, evaluated at $\mathbf{b}$. The vector $\mathbf{b}$ consists of the n individual FORM reliability indexes $\mathbf{b} = \left[\beta'_{d_1}; \ldots, \beta'_{d_i}; \ldots; \beta'_{d_n}\right]$ associated with the different durations. The elements of $\boldsymbol{\rho}$, which describe the correlation between the flood exceedance events $\left\{Q_{d_i}\left(\mathrm{X}_{d_i}\right) > q\right\}$ and $\left\{Q_{d_k}\left(\mathrm{X}_{d_k}\right) > q\right\}$, are calculated based on the random variables $\boldsymbol{\alpha}_{d_i}\mathbf{U}$ as:

$$\rho_{ik} = \boldsymbol{\alpha}_{d_i}\boldsymbol{\alpha}_{d_k}^{\mathrm{T}} \tag{19}$$

For implementation purposes, it is pointed out that Eqs. (18-19) require the different limit state functions $g_d(\mathbf{X}_{\boldsymbol{d}})$ of the individual rainfall durations $d = d_i$ to be defined in the joint space of all random variables, i.e. $g_{d_i}(\mathbf{X})$, with $\mathbf{X} = \left[\mathbf{X}_{d_1}, \ldots, \mathbf{X}_{d_n}\right]$. The reason lies in the correlation $\mathbf{R}_{\mathbf{X}}$, which is included in the transformation from $\mathbf{X}$ to $\mathbf{U}$ (see appendix). The limit state function g_{d_i} is still a function of $\mathbf{X}_{d_i}$ only, i.e. the flood exceedance in duration d_i is fully determined by $\mathbf{X}_{d_i}$ and the hydrological model. However, due to the correlation, the corresponding limit state function G_{d_i} in standard normal space is a function of all variables in $\mathbf{U}$, because the correlations among the $\mathbf{X}$ are included in the transformation and hence in the G_{d_i}'s (the $\mathbf{U}$ are uncorrelated).

2.4.4 Inverse FORM

In many instances, the interest is in solving the inverse problem of determining the discharge q_T that is associated with a fixed return period T or exceedance frequency $1/T$, Eq. (3). If there were only a single relevant rainfall duration d, the inverse problem could be solved in analogy to [*Winterstein et al.*, 1993]. One first identifies the reliability index β_T corresponding to the return period T as $\beta_T = -\Phi^{-1}(1/T)$, with Φ^{-1} being the inverse standard normal CDF. The discharge q_T is then found by solving the optimization problem

$$q_T = \arg\max Q_d[T^{-1}(\mathbf{u}_{\boldsymbol{d}})] \quad \text{subject to} \quad \|\mathbf{u}_{\boldsymbol{d}}\| = \beta_T. \tag{20}$$

In practice, multiple rainfall durations will be of relevance, but the solution of Eq. (20) nevertheless provides a first (non-conservative) indication of the design flood.

To consider multiple rainfall durations, the FORM system problem is solved repeatedly for different values of q. The design flood is then found iteratively. Because of the small computational cost associated with a single FORM run, this is easily implemented.

2.5 Design charts

To facilitate the implementation of the FORM system analysis in engineering practice, we propose the use of *design charts*. In a nutshell, a design chart specifies the representative design storm events, i.e. parameter combinations in function of the desired discharge return period T, which, if used with the traditional design storm approach, replicate the results of the Probabilistic Design Storm approach. A similar idea of calibrating the input parameters of the design storm approach to match the results of a more sophisticated approach has been proposed by [*Camici et al.*, 2011] using continuous simulations.

An exemplary design chart, based on the case study (Section 3.2.8), is shown in Figure 4. As an example, the most likely combination of model parameters that lead to a 100-year discharge are a 90-year rainfall and an 87 quantil of CN. These charts are constructed such that one does not need to know the critical duration. Instead, the 90-year rainfall of different durations is applied to the hydrological model and the maximum peak discharge of the different durations is selected as representative, as is common in the standard design storm approach.

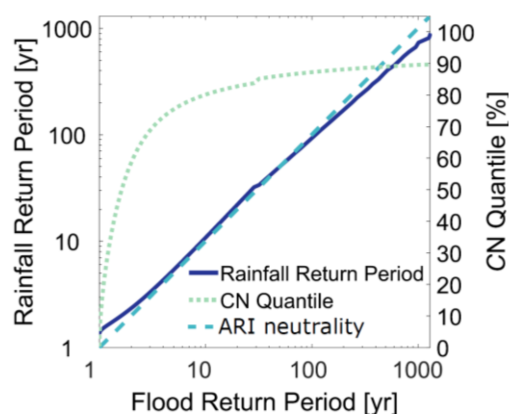

Figure 4. Design chart for the Trauchgauer Ach: Representative design storm events (i.e. recommended combinations of rainfall return periods and CN quantiles) that reproduce the results of the Probabilistic Design Storm method.

The design charts are developed based on the FORM design points $\mathbf{u}_d^*$, since these are the most likely parameter combinations leading to a discharge q_T of return period T. Hence they correspond to the best representative scenario for q_T. This philosophy is in analogy to the partial safety factor concept used in structural engineering [*Sørensen et al.*, 1994]. However, because of the multiple rainfall durations, it is not possible to directly utilize the design points, which are always associated with a single rainfall duration. The following procedure is therefore applied to compute representative parameter combinations $\mathbf{x}_T$.

The basis of the procedure are the flood exceedance probabilities $\Pr(Q(\mathbf{X}) > q)$ for different values of q computed under Section 2.4.4, which provide the discharges q_T associated with a return period T. For a value of q_T, the rainfall duration d with the highest exceedance probability $\Pr(Q_d(\mathbf{X}_d) > q_T)$ is identified (based on the available FORM computations). The corresponding design point $\mathbf{u}_d^*$ is then taken as representative for this return period T. To obtain the representative parameter combinations $\mathbf{x}_T$, $\mathbf{u}_d^*$ is transformed back to the original outcome space (following Eq. (11) for independent random variables).

The design charts then specify quantiles or return periods of the representative parameter combinations $\mathbf{x}_T$ which are to be used as inputs to the traditional design storm approach, as a function of the desired flood return period T. Regionalizing these charts could contribute to improved design flood estimations in engineering practice.

2.6 Rainfall-runoff model utilized in the case study

The proposed methodology can be combined with any event-based rainfall-runoff model. To model the rainfall-runoff relationship in the subsequent case study, the SCS Curve Number (CN) approach [*US Department of Agriculture*, 2004] is used for the runoff generation and an unit hydrograph after [*Wackermann*, 1981] for the runoff concentration. We use these conceptually simple models due to their widespread application in engineering practice for design flood estimations in ungauged basins. Additional details of these models can be found in the appendix.

3 Numerical investigations

3.1 Case Study

The proposed methodology is applied in a case study of an alpine catchment in Germany. The Trauchgauer Ach catchment in southern Bavaria is part of the Lech watershed, it is depicted in Figure 5. Additionally shown are the CN values in the catchment based on the EGAR map (Einzugsgebiete Alpiner Regionen, engl. Catchments in Alpine Regions) [*BLFU*, 2014]. The EGAR map presents the CN_{II} for different hydrotopes in the alpine region, which were derived with irrigation experiments. The main hydrotopes of the Trauchgauer Ach are mixed alpine forests, alpine pastures and hay meadows [*BLFU*, 2014]. The catchment's elevation ranges from 780 m.a.s.l. to 1520 m.a.s.l.

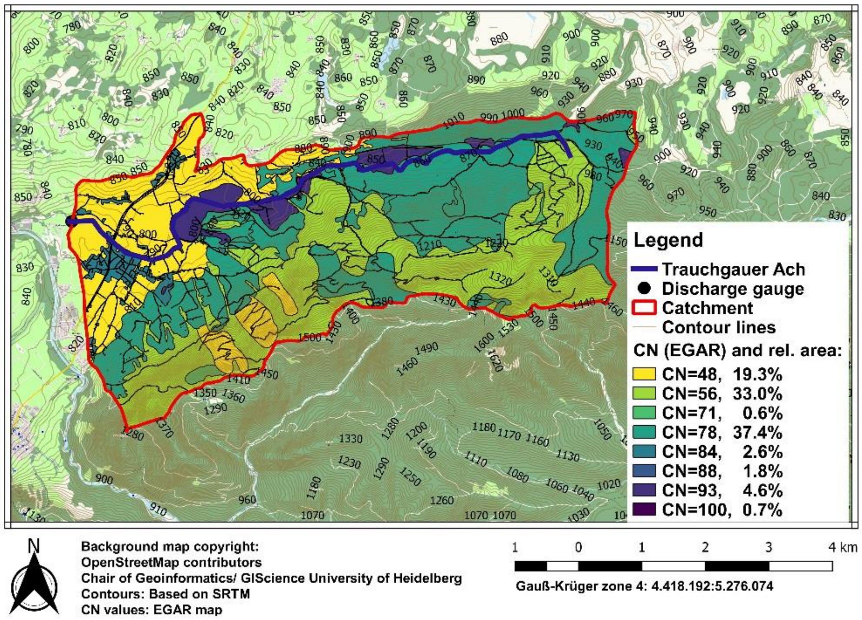

Figure 5. The Trauchgauer Ach catchment [*BLFU*, 2017a]. Background map [*OpenStreetMap contributors*, 2017], contours based on [*NASA*, 2017], CN values from EGAR map [*BLFU*, 2014].

A 90 year record of daily maximum discharges at the gauge Trauchgauer Ach is provided by [*BLFU*, 2017b]. The stream flow data enables a comparison of the proposed Probabilistic Design Storm method to a statistical flood frequency analysis. Additionally, 19 years of precipitation measurements in 1 h discretization at rain gauges Hohenpeißenberg and Bamberg [*DWD*, 2015] allow to estimate the correlation matrix $\mathbf{R_X}$ of the input parameters.

The catchment characteristics are summarized in Table 1 together with the parameters of the unit hydrograph after Wackermann (see appendix).

Table 1. Geomorphological characteristics of the Trauchgauer Ach and the parameters of the Wackermann unit hydrograph (UH) [*Kokolsky*, 2015; *Mrowietz*, 2017].

Geomorphological characteristics		**UH Parameters**	
Area A	$26.7\ km^2$	β	0.20
Flow length L	$14.2\ km$	K_1	0.25
Channel density	$3.7\ km/km^2$	K_2	3.60
Slope I	0.047	-	-

A sensitivity study was carried out to identify important random input parameters for the considered hydrological model [*Berk*, 2015]. It was found that, in addition to the rainfall depths R_d, only uncertainties in CN have a considerable impact on the discharge probabilities. CN represents the catchment conditions that influence the amount of total rainfall transformed to effective rainfall with Eq. (A7). The uncertainty in CN is associated with the variability in the antecedent runoff condition (ARC), which combines the effects of antecedent rainfall, soil moisture conditions, vegetation cover density and stage of growth, and temperature [*US Department of Agriculture*, 2004]. Additional parameter uncertainties that were examined in the sensitivity study are: The temporal rainfall pattern, a model error and statistical uncertainties in the rainfall distribution parameters. All of these input uncertainties had little impact on the discharge frequencies. Therefore, only the rainfall depth and the CN are considered as random variables in the following.

The probabilistic model of annual extreme rainfall depths R_d of different durations is derived from depth-duration-frequency (DDF) curves provided in the Kostra Atlas [*DWD*, 2009]. A shifted exponential distribution is used, whose CDF is

$$F_{R_d}(r_d) = 1 - e^{-\left(\frac{r_d - u_d}{w_d}\right)}, \tag{21}$$

where R_d is the annual maximum rainfall depth of duration d in mm, u_d and w_d are the location and scale parameter of the exponential distribution. The shifted exponential distribution is selected because it is the model underlying the DDF curves in the Kostra Atlas [*Malitz*, 2005]. Parameters of the probabilistic model for different durations are given in Table 2. All rainfall durations given in Table 2 are considered in the case study.

Table 2. Parameters of extreme rainfall depth distributions fitted to the Kostra data for different durations d_i.

Duration d [h]	Location u_d [mm]	Scale w_d [mm]	Mean μ_{rd} [mm]	Standard deviation σ_{rd} [mm]
1	21.00	8.47	29.46	8.47
2	25.80	9.82	35.62	9.82
3	29.10	10.68	39.78	10.68
4	31.74	11.36	43.10	11.36
6	35.80	12.38	48.17	12.38
9	40.37	13.49	53.86	13.49
12	44.01	14.33	58.34	14.33
18	49.50	17.48	66.99	17.48
24	55.00	20.63	75.63	20.63
48	80.00	24.97	104.97	24.97
72	90.00	27.14	117.15	27.14

An area averaged curve number for normal antecedent runoff conditions $CN_{II} = 65.8$ is determined for the catchment from the EGAR map (see Figure 5) in [*Kokolsky*, 2015]. Next, as recommended in [*US Department of Agriculture*, 2004], CN is treated as a random variable, whose median is CN_{II}

and whose 10 % and 90 % quantiles are CN_I and CN_{III}, respectively. For this purpose, $CN_I = 45.2$ and $CN_{III} = 83.1$ are derived with Eqs. (A8) and (A9). A Beta distribution is fitted to these CN values which are typically available in ungauged basins. The resulting distribution is presented in Figure 6a. For simplicity and to be applicable in ungauged basins, this distribution is assumed to be valid for all CN_d of the different moving window durations $d = 1$ h, … , 72 h.

In an ungauged basin, one cannot easily evaluate this modeling assumption, but here we can estimate empirical CN distributions by combining the data from discharge gauge Trauchgau with the rain gauge Hohenpeißenberg to obtain 19 years of concurrent rainfall-runoff events. The derived empirical CN-values are based on the storm events that cause the annual rainfall maxima of different moving window durations and are thus also associated with a duration, as explained in Section 2.2. Figure 6b shows that the beta-CDF fitted to CN_I, CN_{II} and CN_{III} is centered among the empirical CN-value distributions of the different durations. Figure 6c shows that the fitted beta CDF matches the mean empirical CN distribution, which is obtained by averaging over all durations. This demonstrates that the simple probabilistic model of CN is appropriate in the investigated catchment.

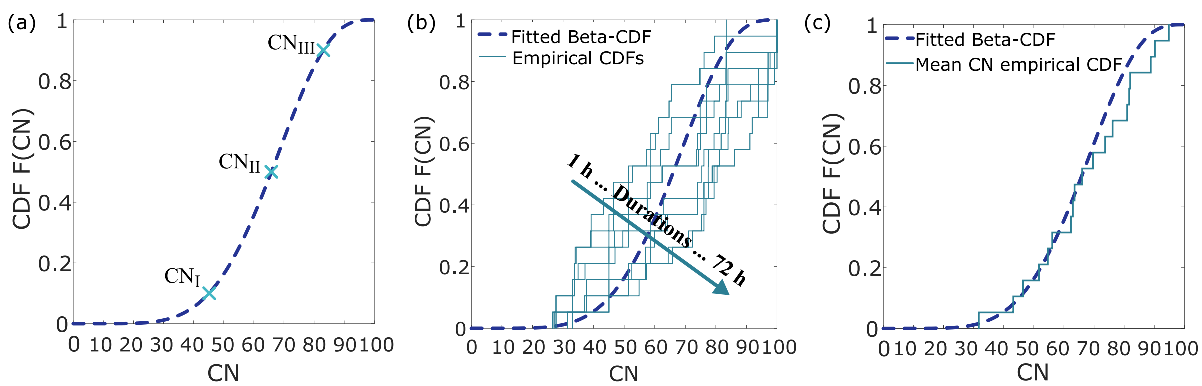

Figure 6. (a) Cumulative distribution function (CDF) of the beta distribution fitted to the CN_I, CN_{II} and CN_{III} values. (b) Comparison of fitted-beta CDF with empirical CN-value distributions of different durations at the Trauchgauer Ach. (c) Empirical CDF of mean CN obtained by averaging the CNs of (b) over all durations.

After transformation of the total rainfall into effective rainfall with the CN, the precipitation is distributed over time with the middle peaked rainfall pattern recommended in [*DVWK*, 1984]. The effect of uncertainty on the temporal rainfall pattern was found to be small [*Berk*, 2015], which justifies the use of a single pattern in the analysis. Due to the small catchment size of 26.9 km^2, no areal reduction of design storms has been taken into account. The base flow is assumed to be constant and is therefore neglected.

3.2 Results

3.2.1 Design flood estimation with the standard design storm (SDS) method

For comparison, the 10-, 100- and 1000-year discharges are calculated using the SDS. Rainfall depths are selected for all rainfall durations from the depth-duration-frequency relationships provided by the Kostra Atlas. The peak discharges are then calculated with the hydrological model for all durations, once using $CN_{II} = 65.8$ for normal conditions and once using $CN_{III} = 83.1$ for wet conditions. For each return period and CN value, the duration with the largest peak discharge is identified and selected as the representative critical duration. Table 3 shows the results of the analysis. The critical rainfall durations are 24 and 48 hours.

Table 3. Results of the standard design storm method.

Curve Number	10-year discharge [m³/s]	Critical duration [h]	100-year discharge [m³/s]	Critical duration [h]	1000-year discharge [m³/s]	Critical duration[h]
CN_{II}	21.8	48	37.0	48	54.4	24
CN_{III}	32.6	48	52.6	24	74.3	24

3.2.2 Probabilistic Design Storm (PDS) method for a single rainfall duration (48 hours)

This section presents the results of the design flood estimation for $d = 48$ h. This duration is selected because it is the critical duration for the 100-year event in the analyzed catchment according to the standard design storm approach (see Section 3.2.1). The relevant uncertain input parameters are $\mathbf{X}_{48} = [CN_{48};\ R_{48}]$, the 48-hours rainfall depth R_{48} and the corresponding CN_{48}. The following results are obtained using the procedure of Sections 2.1 and 2.4.1.

The exceedance probability is evaluated for varying discharge values q. Exemplarily, Figure 7a shows the limit state surfaces (LSS) associated with $= [1; 44; 90]\ \mathrm{m}^3/\mathrm{s}$. These LSS correspond to the combinations of values of CN_{48} and R_{48} that lead to the discharge q. Figure 7b shows the LSS for $q = 44\ \mathrm{m}^3/\mathrm{s}$ in standard normal space, together with the design point and the linearized LSS used in FORM. Transforming this design point back to the space of the original random variables results in the design point on the $q = 44\ \mathrm{m}^3/\mathrm{s}$ LSS shown in Figure 7a. It is reminded that the design point represents the most likely combination of the input parameters that leads to the given discharge. For example, the discharge of 44 m³/s in duration $d = 48$ h is most likely caused by a rainfall of 181 mm and CN equal to 80.

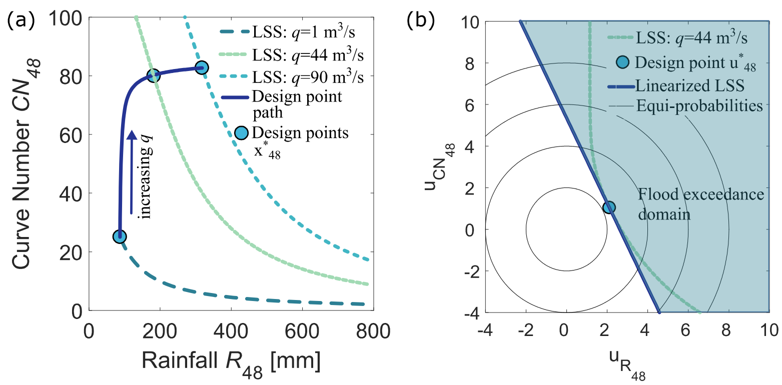

Figure 7. (a) Limit state surfaces (LSS) and design points for critical duration $d = 48$ h for multiple flood magnitudes q in original space. (b) LSS of $q = 44\ \mathrm{m^3/s}$ in standard normal (U-) space with the linearization of the LSS at the design point.

The estimated exceedance probabilities for all evaluated discharges are plotted in Figure 8a. To check the accuracy of the FORM approximation, additionally a Monte Carlo simulation (MCS) with 10^6 samples is performed. As evident from Figure 8a, FORM results in accurate exceedance probabilities. With two random variables $\mathbf{X}_{48} = [CN_{48};\ R_{48}]$, FORM requires between 20-150 model calls to find the design point with Eq. (13) and hence to obtain the exceedance probability for one value of q.

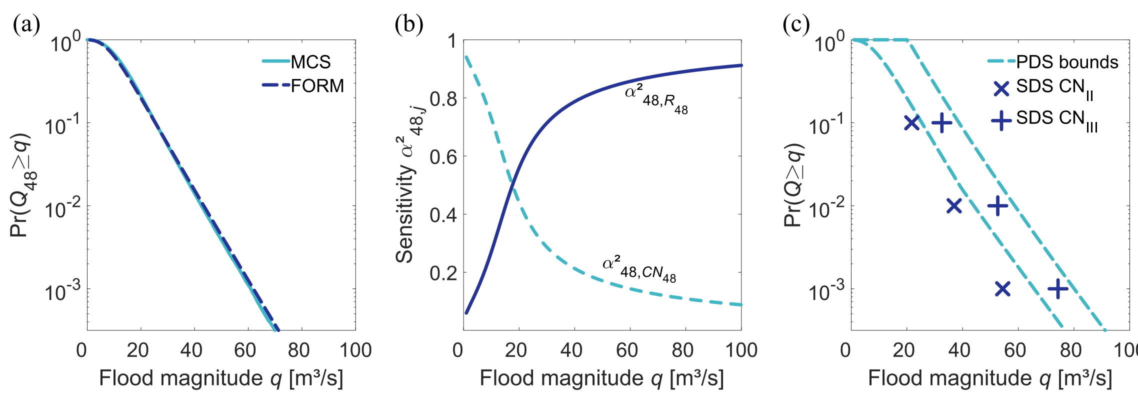

Figure 8. (a) Flood exceedance probabilities for the critical duration $d = 48$ h, comparison of solutions obtained with FORM and MCS. (b) Sensitivity measures $\alpha^2_{48,R_{48}}$ and $\alpha^2_{48,CN_{48}}$ of the flood exceedance probability in function of the flood magnitude q. (c) Probabilistic Design Flood (PDS) bounds on flood exceedance probabilities. Results from the standard design storm (SDS) method utilizing CN_{II} and CN_{III} are shown for comparison.

Besides its computational benefits, a major advantage of FORM is that it provides the location of the design points, i.e. the most likely combination of input parameters leading to a given discharge, as well as sensitivity measures $\alpha_{d,j}$. These sensitivity measures are plotted in Figure 8b as a function of the flood magnitude q. They indicate that low flood magnitudes $q < 20\ \mathrm{m^3/s}$ are more sensitive to the uncertainty in the CN_{48} value and large flood magnitudes $q > 20\ \mathrm{m^3/s}$ are more sensitive to the rainfall depth R_{48}. The same conclusion can be made by comparing the design points associated with different values of q that are displayed by the solid line in Figure 7a: for low discharges, mostly the antecedent runoff conditions of the catchment determine the magnitude of the flood event. For larger floods, the catchment must be already wet, as indicated by a high CN_{48} value, and it is mostly the rainfall that determines the flood magnitude.

3.2.3 Results for different durations

The results of the previous section are here extended to multiple rainfall durations, to compare the flood exceedance probabilities $\Pr\left(Q_{d_i}\left(\mathbf{X}_{d_i}\right) > q\right)$ for different durations d_i.

Table 4 summarizes the return periods $T = 1/\Pr\left(Q_{d_i}\left(\mathbf{X}_{d_i}\right) > q\right)$ associated with the discharge $q = 44\ \mathrm{m^3/s}$ in the different rainfall durations. Among the durations shown here, $d = 24$ h leads to the lowest return period. However, also 6 h and 48 h rainfall durations lead to a non-negligible probability of a flood discharge in excess of $44\ \mathrm{m^3/s}$. The 100-yr flood levels associated with the different durations are also summarized in Table 4. The discharge $q = 44\ \mathrm{m^3/s}$ is the 100-year discharge associated with duration $d = 24$ h. In the full analysis presented later, additional rainfall durations are considered following Table 2.

Table 4. Return periods of a flood magnitude $q = 44\ \mathrm{m^3/s}$ associated with different rainfall durations and 100-year flood levels $q_{T=100yr}$ associated with different rainfall durations.

Rainfall duration	1 h	4 h	6 h	12 h	24 h	48 h	72 h
Return period of $q = 44\ \mathrm{m^3/s}$	225 yr	740 yr	150 yr	217 yr	100 yr	107 yr	340 yr
100-year flood levels $q_{T=100\mathrm{yr}}$	36 $\mathrm{m^3/s}$	30 $\mathrm{m^3/s}$	41 $\mathrm{m^3/s}$	35 $\mathrm{m^3/s}$	44 $\mathrm{m^3/s}$	43 $\mathrm{m^3/s}$	37 $\mathrm{m^3/s}$

3.2.4 Probabilistic Design Storm (PDS) bounds accounting for the effect of different durations

The results obtained for the individual rainfall durations are combined to determine the bounds on design floods following Section 2.3. In calculating these bounds, we model the input parameter $\mathbf{X}_d = [CN_d;\ R_d]$ of a single duration as independent, because information on the correlation between these variables is not commonly available in practice. This assumption is investigated in Section 3.2.6.

Figure 8c presents the bounds on the exceedance probability for the Trauchgauer Ach catchment following Eq. (6). These limit $\Pr(Q(\boldsymbol{X}) > q)$ while accounting for all durations when the correlation $\boldsymbol{\rho}$ of the different exceedance events $\left\{Q_{d_i}\left(\mathbf{X}_{\boldsymbol{d_i}}\right) > q\right\}$ is unknown. Exemplarily, the bounds for the 100-year flood discharge are 45 and $59\ \mathrm{m^3/s}$. To obtain these results with FORM, between 20-150 model evaluations are required for each considered duration d_i and discharge value q.

Figure 8c additionally displays the results obtained with the standard design storm approach (SDS) following section 3.2.1. A comparison of the SDS with CN_{II} for normal antecedent conditions with the PDS bounds clearly shows that the SDS underestimates flood exceedance probabilities. The underestimation of the 100-year flood is between -18 % (relative to the lower bound) and -37 % (relative to the upper bound). If the design storm approach is applied with CN_{III} (representing wet antecedent conditions), both the 100-year and the 1000-year flood estimates for the Trauchgauer Ach lie within the PDS bounds.

To understand the degree to which these results can be generalized, a sensitivity study was conducted, in which the area averaged *CN* value is modified [*Berk*, 2015]. Its main findings are that the underestimation of the design flood with the SDS approach becomes more severe as the average *CN* is reduced. This result is in line with [*Viglione et al.*, 2009] and [*Li et al.*, 2014], who found that for dry catchments (high rainfall abstractions, corresponding to a low CN) the uncertainty in the runoff coefficient (here represented through CN) has a larger influence than for wet catchments with generally low rainfall abstractions. In all cases, the standard design storm approach led to design floods below the lower bound when applying it with CN_{II}, but gave values within the bounds when applying it with CN_{III}.

The upper and lower PDS bounds in Figure 8c give limits on design floods including parameter uncertainties and the effect of different rainfall durations when no information on the dependence between CN_d and R_d are available (i.e. under the assumption of independent CN_d and R_d). The lower bound corresponds to the assumption of fully dependent exceedance events $\{Q_{d_i}(\mathbf{X}_{\boldsymbol{d_i}}) > q\}$ among different durations, so that the critical duration completely determines the exceedance probability, in analogy to the SDS approach. The difference between the lower bound and the results of the SDS approach therefore quantifies the effect of including the uncertainty in the CN instead of using a fixed CN value. The effect of accounting for different rainfall durations and the full correlation structure $\mathbf{R_X}$ of all input parameters $\mathbf{X}$ is presented in the next section.

3.2.5 Probabilistic Design Storm (PDS) estimation including correlation among different durations

The PDS bounds shown in Figure 8c provide an initial estimate of design flood discharge q_T, but they remain quite wide. To compute a single estimate of q_T, the design flood problem is solved jointly for all durations. In this computation, the input parameter vector $\mathbf{X} = [CN_1, \ldots, CN_{72}, R_1, \ldots, R_{72}]$ consists of all CN_d and R_d. The dependence among the input parameters of different durations, described by the correlation matrix $\mathbf{R_X}$, must be included explicitly following Section 2.4.3. In this section, we first study the effect of the correlation among rainfalls of different durations. Thereafter, the cross-correlation in CN_d and the correlation in CN_d and R_d are included.

The correlations among annual maximum rainfall depths R_{d_i} and R_{d_k} associated with different durations d_i and d_k are estimated from rainfall data [*DWD*, 2015] at stations Hohenpeißenberg and Bamberg. Station Hohenpeißenberg is located in southern Bavaria with a distance of approximately 25 km to the case study catchment Trauchgau. We here assume that the correlations at Hohenpeißenberg are valid for the case study due to the proximity. Bamberg is situated in northern Bavaria at a distance of 300 km to the Trauchgauer Ach. It is selected to study the effect of varying correlation patterns on the result.

The annual maximum rainfall depths are extracted from the rainfall data with the moving window approach following Section 2.2. We then compute linear correlation coefficients between any two annual maximum rainfall series of varying durations. In Figure 9, the resulting correlation matrices between the annual maximum rainfall depths R_d of different durations $d = 1, \ldots, 72\ h$ are displayed for rain gauges Hohenpeißenberg and Bamberg. As expected (see Section 2.2), similar rainfall durations are strongly dependent. Overall, the correlation is larger at rain gauge Bamberg (Figure 9b) than at gauge Hohenpeißenberg (Figure 9a), which might be due to the alpine influence at the latter location.

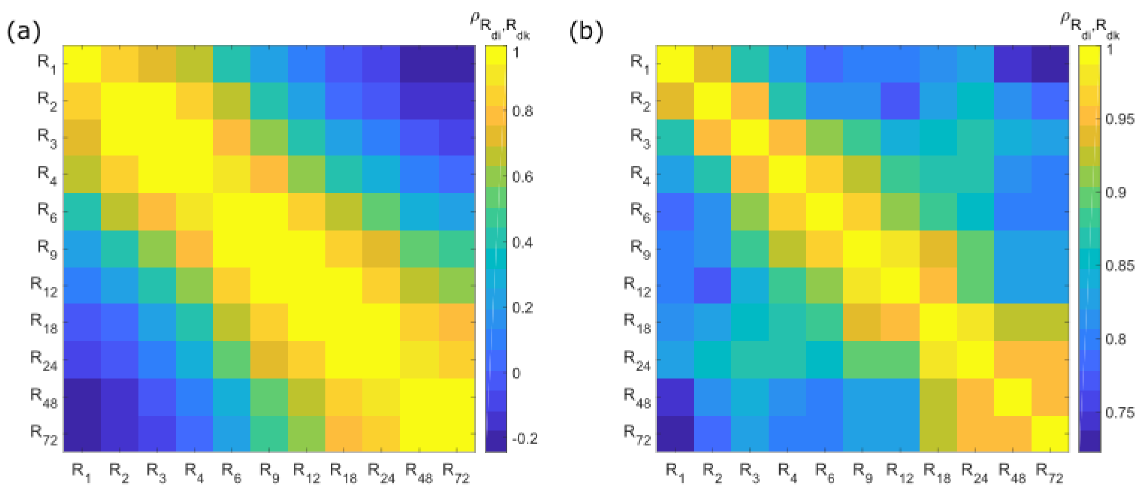

Figure 9. Empirical matrices of linear correlation coefficients of annual maximum rainfall depths R_d of different durations $d = 1, \ldots, 72$ h at (a) Hohenpeißenberg and (b) Bamberg. The colormaps have different scales.

To perform the FORM analysis according to Section 2.4.3, the corresponding correlation matrix has to be transformed to standard normal space (see appendix). As the transformation according to Eq. (A2) however depends on the marginal rainfall distributions, which are here derived from the Kostra Atlas and not based on the rainfall data, a rank-based transformation is utilized to obtain the corresponding correlation in standard normal space [*Song*, 2007].

To study the effect of the rainfall correlation separately from the effect of correlations among other input variables, we first compute results based on a single CN random variable that is applied to all durations d and that is modeled as being independent of rainfall depth R_{d_i}. Rainfall correlations are modelled according to Figure 9. In this computation, the full parameter vector is $\mathbf{X}_{lim} = [CN, R_1, \ldots, R_{72}]$. This model is in analogy to the SDS, which utilizes the same CN_{II} for all durations. It also reflects the situation in many applications, where information is available neither on CN values for different durations nor on their correlations with rainfall depth. The resulting correlation matrices on $\mathbf{X}_{lim}$ based on Figure 9 are denoted with $\mathbf{R}_{\mathbf{X},\text{Hohenp.}}$ and $\mathbf{R}_{\mathbf{X},\text{Bamberg}}$.

In the FORM analysis, the transformation of the correlated inputs $\mathbf{X}_{lim}$ to uncorrelated standard normal space is performed with the Nataf transformation (see appendix). This requires the correlation matrices $\mathbf{R}_{\mathbf{X},\text{Hohenp.}}$ and $\mathbf{R}_{\mathbf{X},\text{Bamberg}}$ of the input random variables $\mathbf{X}_{lim}$ to be positive definite. Due to the randomness in the data, the obtained correlation matrices $\mathbf{R}_{\mathbf{X},\text{Hohenp.}}$ and $\mathbf{R}_{\mathbf{X},\text{Bamberg}}$ including the rainfall correlation of Figure 9 are not positive definite. This is a common problem and solutions to find corresponding positive definite matrices are described in the literature [*Rousseeuw and Molenberghs*, 1993]; here we apply the Eigenvalue method.

Figure 10 shows the resulting Probabilistic Design Storm (PDS) flood exceedance probabilities $\Pr(Q(\mathbf{X}) > q)$ for the Trauchgauer Ach. Despite the fact that the correlation matrices of the annual maximum rainfall depths R_d associated with stations Bamberg and Hohenpeißenberg differ significantly, the resulting flood exceedance probabilities are fairly similar. Bamberg's larger correlation coefficients lead to flood exceedance probabilities that are slightly closer to the lower design flood bound than those obtained with Hohenpeißenberg's correlation matrix.

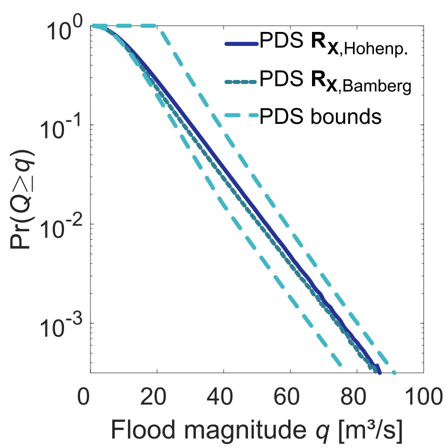

Figure 10. Computed Probabilistic Design Storm (PDS) flood exceedance probabilities accounting for correlation in rainfalls of different durations together with the PDS bounds of Figure 8c.

3.2.6 Probabilistic Design Storm (PDS) estimation including correlation among all input parameters

For the full analysis, the correlation among all random variables $\mathbf{X} = [CN_1, \ldots, CN_{72}, R_1, \ldots, R_{72}]$ is needed as an input. In this case study, these include the cross-correlations among the CN_d as well as the correlation of CN_{d_j} and rainfall depth R_{d_k} for all duration pairs j, k, in addition to the correlation matrices of Figure 9. These correlations cannot be readily derived from the rainfall data alone. Either one needs a continuous simulation to estimate the wetness conditions in the catchment, or the correlation can be estimated based on empirical CN-values derived from concurrent rainfall-runoff events. We follow the latter approach, but point out that this would not be possible in an ungauged basin. The correlations are estimated with the CN_d values of different durations (see also Section 3.1, Figure 6) and the rainfall depths R_d at gauge Hohenpeißenberg. Figure 11a shows the correlation between CN_d and R_d, Figure 11b the cross-correlation in CN_d of different durations. The cross-correlation exhibits a similar pattern as the rainfall correlations in Figure 9, which can be attributed to the fact that in some years the annual rainfall maxima with similar durations are due to the same storm event. It is found that the correlation between CN_d and R_d is mostly negative for low rainfall durations and becomes positive for large rainfall durations.

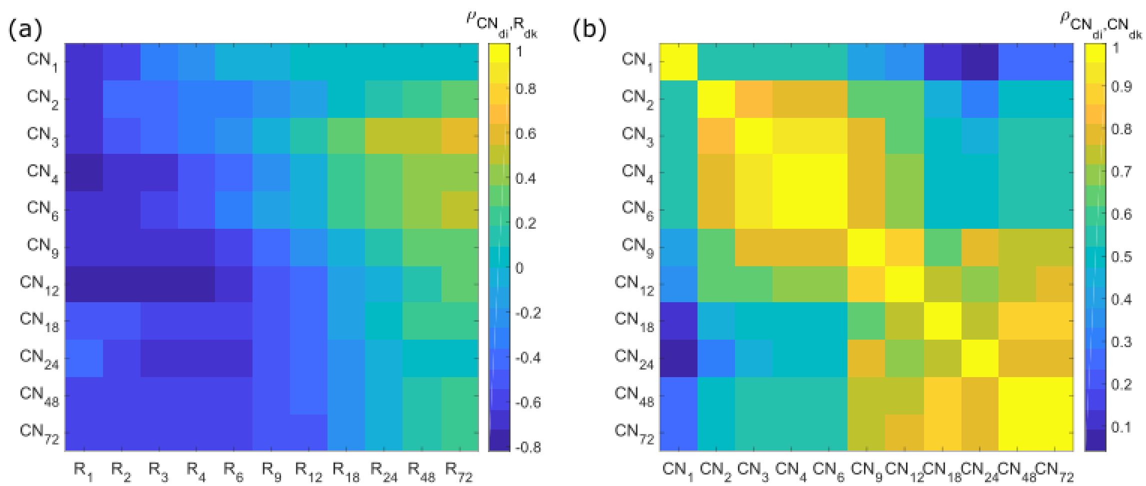

Figure 11. Empirical matrices of linear correlation coefficients of different durations: (a) CN_d and R_d and (b) CN_d and CN_d of different durations $d = 1$ h, … ,72 h at the Trauchgauer Ach. The colormaps have different scales.

Combining the correlations of Figure 11 with the rainfall correlation of gauge Hohenpeißenberg (Figure 9a) gives the correlation matrix $\mathbf{R}_{\mathbf{X},\mathrm{Complete}}$ of all inputs $\mathbf{X} = [CN_1, \dots, CN_{72}, R_1, \dots, R_{72}]$. The results of the Probabilistic Design Storm (PDS) method according to Section 2.4.3 with this complete correlation matrix $\mathbf{R}_{\mathbf{X},\mathrm{Complete}}$ are illustrated in Figure 12. These results required between 200-2000 model evaluations for each duration d_i (here 11 durations) and discharge value q.

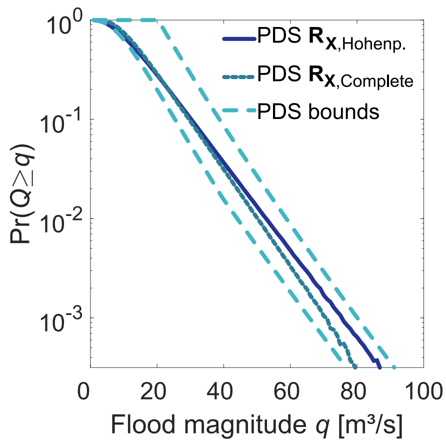

Figure 12. Computed Probabilistic Design Storm (PDS) flood exceedance probabilities accounting for correlation in all input parameters (PDS $\mathbf{R}_{\mathbf{X},\text{Complete}}$) together with the PDS bounds of Figure 8c and the results PDS $\mathbf{R}_{\mathbf{X},\text{Hohenp.}}$ of Figure 10.

The results obtained with the complete dependence structure $\mathbf{R}_{\mathbf{X},\text{Complete}}$ stay within the PDS bounds that assume independence between CN_{d_i} and R_{d_k}, and they are close to the results obtained when accounting only for correlation in rainfall, i.e. with $\mathbf{R}_{\mathbf{X},\text{Hohenp.}}$. For the Trauchgauer Ach catchment, the latter PDS results with $\mathbf{R}_{\mathbf{X},\text{Hohenp.}}$ accounting only for rainfall correlation are therefore deemed to be accurate enough given the uncertainties in an ungauged catchment. $\mathbf{R}_{\mathbf{X},\text{Hohenp.}}$ is easily obtained in an ungauged catchment, because unlike $\mathbf{R}_{\mathbf{X},\mathbf{Complete}}$, it does not require discharge data or a continuous simulation to estimate correlations involving CN values.

3.2.7 Comparison with flood frequencies of measured discharges

With 90 years of discharge records [*BLFU*, 2017b] at the gauge of the Trauchgauer Ach, a flood frequency analysis is conducted. The generalized extreme value (GEV) distribution is selected among different distribution models. The fitted GEV distribution with its 95 % credible intervals is presented in Figure 13a together with the empirical annual exceedance probabilities at the gauge.

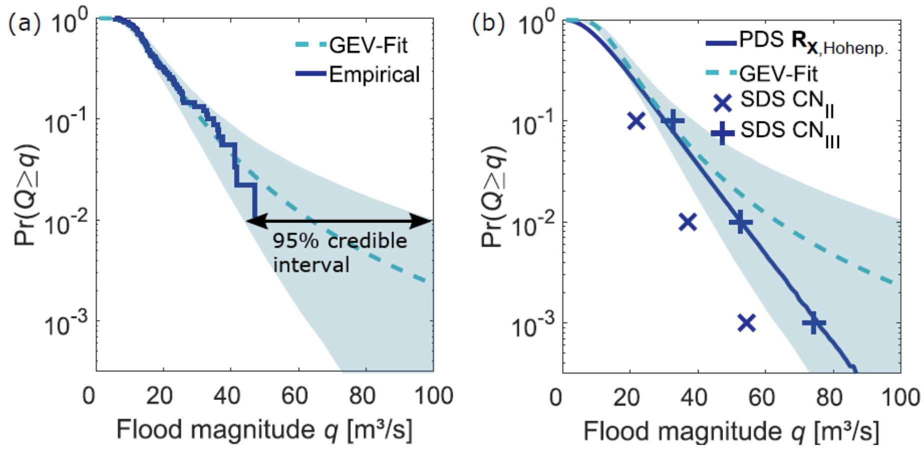

Figure 13. a) Comparison of the empirical flood exceedance probabilities with a GEV distribution fitted to the stream flow data of the Trauchgauer Ach. b) Comparison of the Probabilistic Design Storm method (PDS) and the standard design storm method (SDS) with the GEV distribution.

Figure 13b) compares the Probabilistic Design Storm (PDS) and the standard design storm method (SDS) with the fitted GEV distribution. The results with the PDS method are calculated with the correlation matrix of rainfalls of different durations at gauge Hohenpeißenberg $\mathbf{R}_{\mathbf{X},\mathrm{Hohenp.}}$ (see section 3.2.5).

For large annual exceedance probabilities, the PDS matches well with the statistics derived from stream flow data. For exceedance probabilities below 10^{-2}, the uncertainties in the flood frequency analysis are too large to allow clear conclusions. However, the PDS is within the 95 % credible interval of the flood frequency analysis for the full range of probabilities. The SDS underestimates the design flood, unless CN_{III} is utilized in the computation.

3.2.8 Design Charts: Recommended parameter values for the standard design flood method

The resulting design chart for the Trauchgauer Ach is shown in Figure 4, depicting the representative design storm events. For example, to obtain a flood of return period 100 years with the design storm approach, the 90-year rainfall of the critical duration and the 87% quantile of CN are the most likely parameter combinations causing such a flood event. Similarly, for the 1000-year event it is a 730-year rainfall and a 89% quantile of CN that are most likely to cause such a flood event.

In the range of interest between the 30 and 1000-year flood, the representative CN value is between the 80% - 90% quantile. This is consistent with results shown above, in which the standard design storm approach with CN_{III} (defined as the 90% quantile) leads to design floods that are within the bounds of the Probabilistic Design Storm method. For flood return periods higher than 50 years, the representative value of the rainfall depth is smaller than the $1-\frac{1}{T}$ quantile. A small discontinuity can be observed at a flood return period of around 30 years. This is due to a change of the critical rainfall duration at this point from 48 h to 24 h.

4 Discussion

We have proposed a probabilistic extension of the standard design storm (SDS) method, called Probabilistic Design Storm (PDS) approach, that overcomes the simplification of the SDS while using the same rainfall input data and keeping the computational costs reasonable. The application of the proposed method was demonstrated on a case study using a simple SCS hydrological model. The PDS method can, however, be utilized in combination with any event-based hydrological model and the number of considered uncertain parameters is not limited.

It is well known that the SDS approach tends to underestimate design flood discharges [*Viglione et al.*, 2009; *Grimaldi et al.*, 2012b; *Li et al.*, 2014; *Awadallah et al.*, 2015]. Two reasons can be identified: Firstly, other parameters than the rainfall are also random or uncertain; extreme discharges are associated with large rainfall, but typically also with unfavorable values of other influencing parameters. For this reason, the assumption of ARI neutrality underlying the standard design storm approach does not hold. This is confirmed by the results of the presented case study, which show that the representative design storm event is associated with an 80-90% quantile value of the curve number. This reflects that an extreme discharge event is likely to occur during a period of high antecedent soil moisture. Despite yielding better estimates according to the results presented here, no evidence is found that the CN_{III} (i.e. the 90 % CN-quantile) is used in practice for design flood estimation with the standard design storm method. Instead, [*Pilgrim and Cordery*, 1993] explicitly recommend the use of median values (such as CN_{II}) in the design storm approach to transform the rainfall return period to runoff return period. Also the [*DVWK*, 1984] in Germany recommends the use of CN_{II} for design purposes.

The second reason for the underestimation by the SDS approach is its focus on a single critical rainfall duration, which neglects that, with smaller probability, extreme flood events may be caused by rainfalls of other durations as well. This effect can be appreciated by comparing the result from the analysis considering rainfall correlation with the lower bound in Figure 10. The bounds in Figure 10 do not represent a measure of uncertainty such as a credible or confidence interval. Instead, they represent the two extreme cases of dependence in the exceedance events of different rainfall durations, as explained in Section 2.3. Future work could extend the PDS approach to generate uncertainty intervals on its design flood estimates.

The effect of the different rainfall durations on flood exceedance probabilities depends on the dependence structure of all model input parameters. In most instances, it is possible to obtain data on rainfall, which enables the computation of the correlation among annual maximum rainfalls of different duration, as in Figure 9. In such cases, it is possible to obtain a single estimate of the flood exceedance probability, which neglects statistical dependence associated with the remaining model parameters (Section 3.2.5). In our numerical investigation, this assumption gave result that are sufficiently accurate for most practical applications (Figure 12).

As we demonstrate in Section 3.2.6, the FORM approach enables accounting for the full dependence structure among all input parameters. However, for ungauged catchments, it is generally difficult or impossible to determine the correlations among some of the model parameters (here: CN). Besides the assumptions made in Section 3.2.5, one could also employ correlation structures of catchments with similar characteristics. It is pointed out that, even if some assumptions on correlation structures are necessary in the PDS, the results obtained will still be closer to reality than under the assumption of a single critical duration, as currently utilized in SDS, which is analogue to the lower bound of the PDS estimate.

For the investigated catchment, the underestimation of the SDS compared to the PDS with the complete dependence model is in the order of 28% of the design flood for the 100yr and 22% for 1000yr event. The PDS with simplified dependence structure overestimates the 100yr event by 4% and the 1000yr event by 7%, compared to the full solution (see Figure 12).

For validation purposes, the results of the proposed PDS were compared with a flood frequency analysis of stream flow records. The PDS results closely match the flood frequency analysis while the SDS with CN_{II} is not within the credible interval of the flood frequency analysis. We point out that this is not a proper validation of the method, as the results depend also on the quality of the input probability distributions and the hydrological model. If the probabilistic rainfall input is biased or if the hydrological model does not accurately represent the catchment, errors are introduced that affect both the SDS and PDS. However, we tested the employed hydrological model and the rainfall data, and are confident that they represent a good choice among the simple models available for use in practice for the considered catchment.

The FORM methodology proposed for solving the probabilistic formulation of the design storm problem has two benefits over a Monte Carlo sampling (MCS) approach. Firstly, it is computationally more efficient; however, in combination with simple hydrological models, even a MCS analysis is feasible in practice. Secondly, through identification of the so called design points and calculation of sensitivity indices, the FORM analysis provides additional insights into the parameter combinations that lead to the extreme discharge event, as discussed above. In analogy to semi-probabilistic design concepts used in structural reliability, it allows the identification of representative design storm events, which, if inserted into a deterministic model (here, the SDS method) are representative for design floods of required exceedance probability.

We derived design charts, which summarize these representative design storm events, as a pragmatic tool to utilize the results in practice. An example is shown in Figure 4. These results are strictly valid only for the investigated catchment, but similar results are expected for other catchments. Through investigations of other case studies, it would be possible to find design charts for a specific hydrological model (such as the SCS curve number approach in combination with a unit hydrograph as used here) and for different catchment types. The design charts can help to avoid the error made through the ARI neutrality assumption and consideration of single rainfall duration in the SDS approach. However, it would be better to avoid the SDS approach, and directly employ the PDS approach, which does not require additional input data (unlike e.g. a continuous simulation). The PDS is computationally efficient and it can output the representative design storm events, which facilitate the interpretation of the results by hydrologists that are not experts in probabilistic assessment.

5 Conclusion

We introduced the Probabilistic Design Storm method, which overcomes major limitations of the standard design storm method, namely the assumption of ARI-neutrality and the use of a single critical rainfall duration. The Probabilistic Design Storm method accounts for uncertainty in input parameters other than rainfall, e.g. antecedent wetness, and for multiple rainfall durations. In contrast to continuous hydrological models or probabilistic event-based approaches, the proposed approach only requires the readily available depth-duration-frequency or intensity-duration-frequency (DDF/IDF) curves as input characterizing the extreme rainfall events, which facilitates its implementation to engineering practice. Besides providing an improved design flood estimate, the method also provides sensitivity measures and identifies the most likely combination of input parameters (e.g. of rainfall intensity and antecedent wetness) that cause a design flood with given return period. Such representative design storm events can then be summarized in design charts that can be combined with existing methods for simplified use in engineering practice. The application of the Probabilistic Design Storm method to a small catchment showed that the standard design storm approach significantly underestimates extreme flood discharges.

Acknowledgments, Samples, and Data

We acknowledge insightful discussions and input from Wolfgang Rieger from the Chair of Hydrology at TUM and Simon Mrowietz.

The discharge data as well as EGAR maps for the derivation of the CN-value were kindly provided by Peter Wagner and Andreas Rimböck from the Bavarian Environment Agency (Bayerisches Landesamt für Umwelt). The hourly precipitation data at stations Hohenpeißenberg and Bamberg have been downloaded from Germany's National Meteorological Service (Deutscher Wetterdienst, http://www.dwd.de/). The depth duration frequency information of the rainfall were extracted from KOSTRA-DWD-2000, a service provided by Germany's National Meteorological Service (Deutscher Wetterdienst). Further information on the sources of the data can be found in the reference section.

Olga Spackova acknowledges support by the German Science Foundation (DFG) through the TUM International Graduate School of Science and Engineering (IGSSE).

Appendix

Nataf Transformation

The Nataf transformation is summarized based on [*Der Kiureghian and Liu*, 1986; *Melchers*, 1999]. First, the correlated random variables **X** are marginally transformed to correlated standard normal random variables **Z**:

$$Z_j = \Phi^{-1}[F_{X_j}(X_j)] \tag{A1}$$

where F_{X_j} is the CDF of the random variable X_j and Φ^{-1} is the inverse standard normal CDF.

Next, the correlation $\dot{\rho}_{j,l}$ of the standard normal random variables Z_j and Z_l can be obtained from the correlation matrix $\mathbf{R_X}$ of the random variables **X** through the following equality:

$$\rho_{j,l} = \int_{-\infty}^{\infty}\int_{-\infty}^{\infty} \frac{(x_j - \mu_j)}{\sigma_j} \cdot \frac{(x_l - \mu_l)}{\sigma_l} * \varphi_2(z_j, z_l, \dot{\rho}_{j,l}) dz_j dz_l \tag{A2}$$

where $\rho_{j,l}$ is the correlation of X_j and X_l, φ_2 the bivariate normal PDF, μ_i and μ_j are the means of X_j and X_l, σ_j and σ_l are the corresponding standard deviations. The result is $\mathbf{R}_{\boldsymbol{Z}}$, the correlation matrix of the correlated standard normal random variables **Z**. To avoid evaluating $\dot{\rho}_{j,l}$ through Eq. (A2), approximation formulas have been developed in function of the marginal distribution type [*Der Kiureghian and Liu*, 1986; *Ditlevsen and Madsen*, 1996].

The final step is the transformation of **Z** to uncorrelated standard normal random variables **U**:

$$T_{Nataf}\colon \mathbf{U} = \boldsymbol{L}_{\boldsymbol{z}}^{-\mathbf{1}} \cdot \mathbf{Z} \tag{A3}$$

with $\boldsymbol{L}_{\boldsymbol{z}}$ the lower triangle matrix of a Choleski decomposition of $\mathbf{R}_{\boldsymbol{Z}}$:

$$\mathbf{R}_{\boldsymbol{Z}} = \boldsymbol{L}_{\boldsymbol{z}} \cdot \boldsymbol{L}_{\boldsymbol{z}}^{\boldsymbol{T}} \tag{A4}$$

For FORM, the inverse Nataf transformation is required:

$$\boldsymbol{Z} = \boldsymbol{L}_{\boldsymbol{z}} \cdot \boldsymbol{U} \tag{A5}$$

$$T_{Nataf}^{-1}(\mathbf{U}, \mathbf{R_X})\colon X_j = {F_{X_j}}^{-1}\left(\Phi(Z_j)\right) \tag{A6}$$

${F_{X_j}}^{-1}$ is the inverse CDF of random variable X_j and Φ the standard normal CDF.

SCS Curve Number (CN) approach

For the background on the SCS-CN approach we refer to [*US Department of Agriculture*, 2004; *Mays*, 2005; *Maniak*, 2010]. The relationship between total and effective rainfall in [mm] utilized in this paper is [*DVWK*, 1990, 1991]:

$$R_{eff} = \frac{\left(\frac{R}{25.4} - \frac{50}{CN} + 0.5\right)^2}{\frac{R}{25.4} + \frac{950}{CN} - 9.5} \cdot 25.4 \quad \text{(A7)}$$

with R the total rainfall, R_{eff} the effective rainfall and CN the Curve Number. As recommended in [*DVWK*, 1991] for southern Germany, Eq. (A7) assumes an initial loss of 5 % instead of the original 20 %. It is typically distinguished between CN_{II} for average conditions, CN_I for dry conditions and CN_{III} wet conditions in the catchment [*US Department of Agriculture*, 2004]. The following relation [*Maniak*, 2010] between CN_{II} and CN_I

$$CN_I = \frac{CN_{II}}{2.334 - 0.01334 \cdot CN_{II}} \quad \text{(A8)}$$

and CN_{II} and CN_{III}

$$CN_{III} = \frac{CN_{II}}{0.4036 + 0.0059 \cdot CN_{II}} \quad \text{(A9)}$$

is applied.

Unit hydrograph after Wackermann

The unit hydrograph $h(\tau)$ after Wackermann is based on two parallel storage cascades, one for overland flow and one for interflow [*Wackermann*, 1981]:

$$h(\tau) = \beta \cdot \frac{\tau \cdot \exp(-\frac{\tau}{K_1})}{K_1^2} + (1 - \beta) \cdot \frac{\tau \cdot \exp(-\frac{\tau}{K_2})}{K_2^2} \quad \text{(A10)}$$

The parameters β, K_1 and K_2 are related to the geomorphological characteristics of the catchment [*Wackermann*, 1981; *Harms*, 1986]:

$$\beta = \begin{cases} 0.323 \cdot \exp(-0.00765 \cdot L/\sqrt{I}), & for\ L/\sqrt{I} \leq 454 \\ 0.01, & for\ L/\sqrt{I} > 454 \end{cases} \tag{A11}$$

with L the length of the main flow path from water divide to the gauge in km and I the slope of the main flow path;

$$K_1 = \begin{cases} 4.375 - 2.247 \cdot \gamma, & for\ \gamma \leq 1.836 \\ 0.25, & for\ \gamma > 1.836 \end{cases} \tag{A12}$$

with γ the flow path network density defined by the length of the streams displayed in a 1:25000 topography map in relationship to the catchment area A in km/km^2;

$$K_2 = \begin{cases} 0.067 \cdot L/\sqrt{I}, & for\ L/\sqrt{I} \leq 50 \\ 0.0168 \cdot L/\sqrt{I} + 2.5, & for\ L/\sqrt{I} > 50 \end{cases} \tag{A13}$$

6 References

Arnaud, P., P. Cantet, and Y. Aubert (2015), Relevance of an at-site flood frequency analysis method for extreme events based on stochastic simulation of hourly rainfall, *Hydrological Sciences Journal*, *61*(1), 36–49, doi:10.1080/02626667.2014.965174.

Aronica, G. T., and A. Candela (2007), Derivation of flood frequency curves in poorly gauged Mediterranean catchments using a simple stochastic hydrological rainfall-runoff model, *J. Hydrol. (Journal of Hydrology)*, *347*(1-2), 132–142, doi:10.1016/j.jhydrol.2007.09.011.

Awadallah, A. G., H. Saad, A. Elmoustafa, and A. Hassan (2015), Reliability assessment of water structures subject to data scarcity using the SCS-CN model, *Hydrological Sciences Journal*, n/a, doi:10.1080/02626667.2015.1027709.

Berk, M. (2015), Probabilistic Modeling Of Design Floods Including Parameter Uncertainties, Master's thesis, Engineering Risk Analysis Group, Technical University of Munich, Munich.

Blazkova, S., and K. Beven (2009), A limits of acceptability approach to model evaluation and uncertainty estimation in flood frequency estimation by continuous simulation: Skalka catchment, Czech Republic, *Water Resour. Res.*, *45*(12), n/a, doi:10.1029/2007WR006726.

BLFU (2014), EGAR-Kartierung: Erläuterungen und Beschreibung der Vegetations- bzw. Hydrotop-Typen in Wildbacheinzugsgebieten, Mit CN-Werten und Gesamtabflussbeiwerten und für das SCS-Verfahren (Caspary), Bayerisches Landesamt für Umwelt BLFU, Augsburg.

BLFU (2017a), *Catchment Trauchtgauer Ach*, Bayerisches Landesamt für Umwelt BLFU (Bavarian Environment Agency).

BLFU (2017b), Daily discharge maxima at gauge Trauchgauer Ach.

Calver, A., and R. Lamb (1995), Flood frequency estimation using continuous rainfall-runoff modelling, *Physics and Chemistry of the Earth*, *20*(5-6), 479–483, doi:10.1016/S0079-1946(96)00010-9.

Cameron, D., K. Beven, and P. Naden (2000), Flood frequency estimation by continuous simulation under climate change (with uncertainty), *Hydrol. Earth Syst. Sci.*, *4*(3), 393–405, doi:10.5194/hess-4-393-2000.

Cameron, D., K. Beven, J. Tawn, S. Blazkova, and P. Naden (1999), Flood frequency estimation by continuous simulation for a gauged upland catchment (with uncertainty), *Journal of Hydrology*, *219*(3-4), 169–187, doi:10.1016/S0022-1694(99)00057-8.

Camici, S., A. Tarpanelli, L. Brocca, F. Melone, and T. Moramarco (2011), Design soil moisture estimation by comparing continuous and storm-based rainfall-runoff modeling, *Water Resour. Res.*, *47*(5), doi:10.1029/2010WR009298.

Der Kiureghian, A., and P. Liu (1986), Structural Reliability under Incomplete Probability Information, *J. Eng. Mech.*, *112*(1), 85–104, doi:10.1061/(ASCE)0733-9399(1986)112:1(85).

Der Kiureghian, A. (2005), First- and Second-Order Reliability Methods, in *Engineering design reliability handbook*, edited by E. Nikolaidis et al., p. 14, CRC Press, Boca Raton, Fla.

Ditlevsen, O. (1979), Narrow reliability bounds for structural systems, *Journal of Structural Mechanics*, *7*(4), 453–472.

Ditlevsen, O., and H. O. Madsen (1996), *Structural reliability methods*, 372 pp., Wiley, Chichester.

DVWK (1984), *Arbeitsanleitung zur Anwendung von Niederschlag-Abfluß-Modellen in kleinen Einzugsgebieten: Teil II: Synthese*, VI, 34 S., *DVWK-Regeln zur Wasserwirtschaft*, vol. 113, Parey, Hamburg.

DVWK (1990), *Arbeitsanleitung zur Anwendung von Niederschlag-Abfluß-Modellen in kleinen Einzugsgebieten: Teil II: Synthese*, 2nd ed., *DVWK-Regeln zur Wasserwirtschaft*, vol. 113, Parey, Hamburg.

DVWK (1991), *Hydraulische Berechnung von Fliessgewässern: DK 551.51/54 Fliessgewässer ; DK 532.543 Hydraulik*, VI, 64 S, *DVWK-Merkblätter zur Wasserwirtschaft*, vol. 220, Parey, Hamburg [u.a.].

DWD (2009), *KOSTRA-DWD-2000: Starkniederschlagshöhen für Deutschland*, Deutscher Wetterdienst.

DWD (2015), Climatological time series: hourly sums of precipitation (in mm), ftp://ftp-cdc.dwd.de/pub/CDC/observations_germany/climate/hourly/precipitation/historical/.

Grimaldi, S., A. Petroselli, and F. Serinaldi (2012a), A continuous simulation model for design-hydrograph estimation in small and ungauged watersheds, *Hydrological Sciences Journal*, *57*(6), 1035–1051, doi:10.1080/02626667.2012.702214.

Grimaldi, S., A. Petroselli, and F. Serinaldi (2012b), Design hydrograph estimation in small and ungauged watersheds: continuous simulation method versus event-based approach, *Hydrol. Process.*, *26*(20), 3124–3134, doi:10.1002/hyp.8384.

Haberlandt, U., Ebner von Eschenbach, A.-D., and I. Buchwald (2008), A space-time hybrid hourly rainfall model for derived flood frequency analysis, *Hydrol. Earth Syst. Sci.*, *12*(6), 1353–1367, doi:10.5194/hess-12-1353-2008.

Harms, R. W. (1986), *Auswirkungen der Urbanisierung auf den Hochwasserabfluß kleiner Einzugsgebiete: Verfahren zur quantitativen Abschätzung*, XVIII, 159 S., *Schriftenreihe des Deutschen Verbandes für Wasserwirtschaft und Kulturbau e.V*, vol. 75, Parey, Hamburg [u.a].

Hohenbichler, M., and R. Rackwitz (1981), Non-normal dependent vectors in structural safety, *Journal of the Engineering Mechanics Division*, *107*(6), 1227–1238.

Hohenbichler, M., and R. Rackwitz (1982), First-order concepts in system reliability, *Structural Safety*, *1*(3), 177–188, doi:10.1016/0167-4730(82)90024-8.

Kokolsky, C. (2015), Vergleichende Studie der bayerischen alpinen Einzugsgebiete: Einzugsgebietscharakteristika, Bachelor Thesis, Chair of Hydrology and River Basin Management, Technische Universität München, Munich.

Lamb, R., and A. L. Kay (2004), Confidence intervals for a spatially generalized, continuous simulation flood frequency model for Great Britain, *Water Resour. Res.*, *40*(7), n/a, doi:10.1029/2003WR002428.

Lawrence, D., E. Paquet, J. Gailhard, and A. K. Fleig (2014), Stochastic semi-continuous simulation for extreme flood estimation in catchments with combined rainfall–snowmelt flood regimes, *Nat. Hazards Earth Syst. Sci.*, *14*(5), 1283–1298, doi:10.5194/nhess-14-1283-2014.

Li, J., M. Thyer, M. Lambert, G. Kuczera, and A. Metcalfe (2014), An efficient causative event-based approach for deriving the annual flood frequency distribution, *Journal of Hydrology*, *510*, 412–423, doi:10.1016/j.jhydrol.2013.12.035.

Loukas, A. (2002), Flood frequency estimation by a derived distribution procedure, *Journal of Hydrology*, *255*(1-4), 69–89, doi:10.1016/S0022-1694(01)00505-4.

Loukas, A., M. C. Quick, and S. O. Russell (1996), A physically based stochastic-deterministic procedure for the estimation of flood frequency, *Water Resour. Manage. (Water Resources Management)*, *10*(6), 415–437, doi:10.1007/BF00422548.

Malitz, G. (2005), *KOSTRA-DWD-2000: Starkniederschlagshöhen für Deutschland (1951 - 2000)*, Grundlagenbericht, Deutscher Wetterdienst - Hydrometeorologie, Offenbach am Main.

Maniak, U. (2010), *Hydrologie und Wasserwirtschaft: Eine Einführung für Ingenieure*, 1 online resource (700, Springer Berlin Heidelberg, Berlin/Heidelberg.

Mays, L. W. (2005), *Water resources engineering*, 2005th ed., xv, 842, John Wiley & Sons, New Jersey.

Melchers, R. E. (1999), *Structural reliability analysis and prediction*, 2nd ed., xviii, 437, John Wiley, Chichester, New York.

Melching, C. S. (1992), An improved first-order reliability approach for assessing uncertainties in hydrologic modeling, *Journal of Hydrology*, *132*(1-4), 157–177, doi:10.1016/0022-1694(92)90177-W.

Mrowietz, S. (2017), Design Flood Estimation in Bavarian Alpine (and sub-Alpine) Catchments Including Parameter Uncertainties, Master Thesis, Engineering Risk Analysis Group and Chair of Hydrology and River Basin Management, Technische Universität München, Munich.

NASA (2017), Shuttle Radar Topography Mission (SRTM) Digital Surface Model of Germany, http://www.opendem.info.

OpenStreetMap contributors (2017), OpenStreetMap, University of Heidelberg, Chair of Geoinformatics: WebMapService of World, http://www.osm-wms.de/.

Papaioannou, I., W. Betz, K. Zwirglmaier, and D. Straub (2015), MCMC algorithms for Subset Simulation, *Probabilistic Engineering Mechanics*, *41*, 89–103, doi:10.1016/j.probengmech.2015.06.006.

Paquet, E., F. Garavaglia, R. Garçon, and J. Gailhard (2013), The SCHADEX method: A semi-continuous rainfall–runoff simulation for extreme flood estimation, *Journal of Hydrology*, *495*, 23–37, doi:10.1016/j.jhydrol.2013.04.045.

Pathiraja, S., S. Westra, and A. Sharma (2012), Why continuous simulation? The role of antecedent moisture in design flood estimation, *Water Resour. Res.*, *48*(6), doi:10.1029/2011WR010997.

Pilgrim, D. H., and I. Cordery (1993), Flood Runoff, in *Handbook of hydrology*, edited by D. R. Maidment, p. 9, McGraw-Hill, New York.

Rackwitz, R. (2001), Reliability analysis—a review and some perspectives, *Structural Safety*, *23*(4), 365–395, doi:10.1016/S0167-4730(02)00009-7.

Rackwitz, R., and B. Fiessler (1978), Structural reliability under combined random load sequences, *Computers & Structures*, *9*(5), 489–494, doi:10.1016/0045-7949(78)90046-9.

Rahman, A., P. Weinmann, T. Hoang, and E. Laurenson (2002), Monte Carlo simulation of flood frequency curves from rainfall, *Journal of Hydrology*, *256*(3-4), 196–210, doi:10.1016/S0022-1694(01)00533-9.

Rogger, M., B. Kohl, H. Pirkl, A. Viglione, J. Komma, R. Kirnbauer, R. Merz, and G. Blöschl (2012), Runoff models and flood frequency statistics for design flood estimation in Austria – Do they tell a consistent story?, *Journal of Hydrology, 456-457,* 30–43, doi:10.1016/j.jhydrol.2012.05.068.

Rousseeuw, P. J., and G. Molenberghs (1993), Transformation of non positive semidefinite correlation matrices, *Communications in Statistics - Theory and Methods*, *22*(4), 965–984, doi:10.1080/03610928308831068.

Shaw, E. M., K. J. Beven, and N. A. Chappell (2011), *Hydrology in practice*, 4th ed., xiv, 543, Spon, London, New York.

Song, P. X.-K. (2007), *Correlated data analysis: Modeling, analytics and applications*, XV, 346 ;, *Springer Series in Statistics*, Springer, New York.

Sørensen, J. D., I. B. Kroon, and M. H. Faber (1994), Optimal reliability-based code calibration, *Structural Safety*, *15*(3), 197–208.

Straub, D. (2014), Engineering Risk Assessment, in *Risk - A Multidisciplinary Introduction*, edited by C. Klüppelberg et al., pp. 333–362, Springer International Publishing, Cham.

Svensson, C., T. R. Kjeldsen, and D. A. Jones (2013), Flood frequency estimation using a joint probability approach within a Monte Carlo framework, *Hydrological Sciences Journal*, *58*(1), 8–27, doi:10.1080/02626667.2012.746780.

US Department of Agriculture (2004), Estimation of Direct Runoff from Storm Rainfall: Chapter 10, *National Engineering Handbook Part 630 Hydrology*, Washington, D.C., http://www.nrcs.usda.gov/wps/portal/nrcs/detailfull/national/water/?cid=stelprdb1043063.

Verhoest, N., S. Vandenberghe, P. Cabus, C. Onof, T. Meca-Figueras, and S. Jameleddine (2010), Are stochastic point rainfall models able to preserve extreme flood statistics?, *Hydrol. Process.*, *24*(23), 3439–3445, doi:10.1002/hyp.7867.

Viglione, A., R. Merz, and G. Blöschl (2009), On the role of the runoff coefficient in the mapping of rainfall to flood return periods, *Hydrol. Earth Syst. Sci.*, *13*(5), 577–593, doi:10.5194/hess-13-577-2009.

Wackermann, R. (1981), Eine Einheitsganglinie aus charakteristischen Systemwerten ohne Niederschlag-Abfluss-Messungen, *Wasser und Boden*(H 1), 23–28.

Winterstein, S. R., T. C. Ude, C. A. Cornell, P. Bjerager, and S. Haver (1993), Environmental parameters for extreme response: Inverse FORM with omission factors, in *Proc. 6th Int. Conf. on Structural Safety and Reliability, Innsbruck, Austria*.